

10. DATA REPORT: ORGANIC PETROLOGY OF LEG 180 SAMPLES, WESTERN WOODLARK BASIN, PAPUA NEW GUINEA¹

Alan C. Cook² and Garry D. Karner³

ABSTRACT

Seventy-one samples from Ocean Drilling Program Leg 180 sites were analyzed for vitrinite reflectance and organic type. The objective was to define maximum paleotemperatures across the western Woodlark Basin as a function of depth. The organic matter is of early Pliocene to Holocene age and was recovered from drilled depths of 4.5 to 851.3 meters below seafloor. Organic matter is generally restricted to woody fragments within the sediment, although in a number of fine-grained samples, organic matter is dispersed throughout the sample. Virtually all samples contain vitrinite, part of which may be derived from drifted logs. One sample was found to be barren of organic matter, and two contain only fusinite and semifusinite.

Variation of vitrinite reflectance is not systematic with either depth or location, and it appears that formation temperatures have been insufficient to cause an increase in vitrinite reflectance levels. Textural variations within the vitrinite show better correlation with depth. Samples of hypautochthonous peats represent either a terrestrial phase of sedimentation or large peat intraclasts within the section, possibly produced by forest fires in the source areas of the organic matter. The vitrinite and peat-derived samples appear to come from eucalyptus forest settings away from the coastline. Liptinite is not abundant in most of the samples (excluding suberinite associated with woody tissues). Marine liptinite is rare to absent, although many of the samples contain abundant foraminiferal tests. Pyrite is abundant in many of the wood fragments, and some pyritization of woody tissues has taken place.

¹Cook, A.C., and Karner, G.D., 2002. Data report: Organic petrology of Leg 180 samples, western Woodlark Basin, Papua New Guinea. In Huchon, P., Taylor, B., and Klaus, A. (Eds.), *Proc. ODP, Sci. Results*, 180, 1–35 [Online]. Available from World Wide Web: <http://www-odp.tamu.edu/publications/180_SR/VOLUME/CHAPTERS/157.PDF>. [Cited YYYY-MM-DD]

²Keiraville Konsultants Pty Ltd., 7 Dallas Street, Keiraville NSW 2500, Australia.

³Lamont-Doherty Earth Observatory, PO Box 1000, Palisades NY 10964, USA. garry@ldeo.columbia.edu

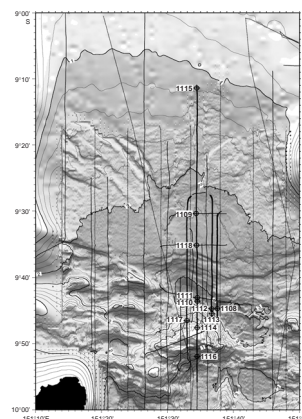
INTRODUCTION

The results of drilling during Ocean Drilling Program (ODP) Leg 180 provided insights into fundamental processes of continental breakup, being part of a westward propagation of a spreading center into continental crust of the western Woodlark Basin, offshore Papua New Guinea (Fig. F1) (Robertson et al., 2001). The Woodlark Basin lies between the D'Entrecasteaux and Louisiade Islands to the southwest and the Trobriand and Woodlark Islands to the northeast. A generally north-south transect of holes was drilled across the western Woodlark region that included the Moresby Seamount (Sites 1114 and 1116), the hanging wall of the low-angle (25° – 30°) extensional Moresby Detachment fault (Sites 1108, 1110–1113, and 1117), and across the collapsed northern rift margin (Sites 1118, 1109, and 1115). The results, when placed in a regional tectonic context, document a history of Paleogene ophiolite emplacement followed by Miocene arc-related sedimentation. Regional uplift and emergence of the forearc area took place in the late Miocene. Submergence to form the Woodlark rift began in the latest Miocene, marked by a widespread marine transgression and shallow-water deposition, accompanied by input of air-fall tephra and volcanoclastic sediments. During the Pleistocene, a carbonate platform was constructed to the northwest, trapping clastic sediment and resulting in a switch to slower, more pelagic and hemipelagic deposition within the Woodlark rift basin.

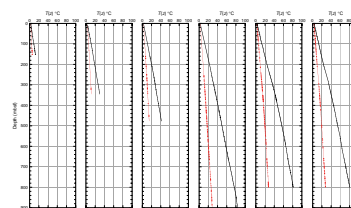
The distribution and amplitude of the large Pliocene–Quaternary regional subsidence across the Woodlark Basin occurs with little attendant brittle deformation. The brittle deformation that does occur, such as movement across the Moresby Detachment fault, represents extension that has occurred over only the last 1 m.y. Driscoll and Karner (1998) have recently advanced an explanation for this paradox in their work from the northwest Australian margin. Here, Tithonian–Valanginian rifting generated large post-Valanginian regional subsidence across the Exmouth Plateau with only minor accompanying brittle deformation and erosional truncation. Based on the stratal relationships and facies distribution, Driscoll and Karner (1998) demonstrated that large portions of the plateau were emergent or at shallow water depths immediately prior to Tithonian–Valanginian extension. To match the distribution and magnitude of the post-Valanginian thermal-type subsidence required significant lower crustal and mantle lithosphere extension across the plateau, implying the existence of an eastward-dipping, intracrustal detachment having a ramp-flat-ramp geometry that allowed preferential thinning of the lower crust and lithospheric mantle. A direct implication of this extension distribution is a significant increase of basal heat flux, which should be represented in sediment temperatures. As we will show, however, sediment temperatures are relatively low, with maximum temperatures $\leq 85^{\circ}\text{C}$ (Fig. F2), with an average temperature significantly less than this value.

Whereas the deformation of the upper crust is relatively simple to constrain using field mapping and potential field and multichannel seismic reflection data, mapping the distribution of lower crustal and lithospheric mantle deformation is difficult. Sediment temperatures and paleotemperatures offer an indirect but crucial tool to map the partitioning of lithospheric extension as a function of depth (Murchison et al., 1985). Unfortunately, relatively shallow sediment lithification across much of the western Woodlark Basin resulted in a paucity of reli-

F1. Bathymetric map showing locations of Leg 180 drill sites, p. 16.



F2. Estimates of thermal gradient and maximum temperatures, p. 17.



able thermal gradient measurements using the Adara and Davis-Vilinger thermal probes. Although estimates of thermal gradient were obtained at five sites during Leg 180, those at Sites 1109 and 1115 were considered unreliable. During Leg 180 drilling, 71 samples containing wood and charcoal fragments were obtained for shore-based vitrinite reflectance work. The sample suite consists of mainly sandy and silty lithologies with relatively minor inclusions of organic matter. These proved to consist of woody fragments preserved as vitrinite, but other macerals are present as well. In some sections, small phytoclasts comprise the major form of organic matter and this mode of occurrence ranges from rare to major (<0.1% to >10% by volume). Water depths at the various drilling sites range from 406.4 to 3177.0 m, all being below the thermocline. It can be assumed that the seafloor temperatures are <4°C for the deeper sites. Even with basal heat fluxes of >100 mW/m², formation temperatures <1 km below the seafloor (i.e., maximum drilling depths) (Taylor, Huchon, Klaus, et al., 1999) only range from 10°–85°C. These temperatures are unlikely to induce any change in coal or vitrinite rank, based on the analysis summarized in Figure F2. Estimates of thermal gradient and maximum temperatures assuming basal heat flux values of 28 and 100 mW/m² estimated from Leg 180 drilling (Taylor, Huchon, Klaus, et al., 1999) and using measured sediment thermal conductivities predicts maximum sediment temperatures of ~85°C.

The objective of this paper is to define the maximum paleotemperatures across the western Woodlark Basin as a function of depth by measuring the vitrinite reflectance and type of organic matter sampled from Leg 180 Holes 1108B, 1109C, 1114A, 1115A, 1115B, 1115C, 1116A, and 1118A (located in Fig. F1).

REGIONAL SETTING

The Woodlark rift is located along the northern periphery of the Papuan Peninsula and the offshore D'Entrecasteaux Islands. The rift basin deepens eastward into the ~500-km-long contemporaneous oceanic Woodlark spreading center (Weissel et al., 1982; Binns and Whitford, 1987; Benes et al., 1994; Goodliffe et al., 1993, 1997; Taylor, Huchon, Klaus, et al., 1999). The spreading tip, located at 9.8°N, 171.7°E, reaches within 1 nmi of the most easterly drill site (Site 1108).

The Woodlark rift is divisible into a relatively narrow (~50 km), deep (~3000 m) fault-bounded rift basin in the south and a wider (~50 km), shallower (~1000–2000 m) northern margin. The Pliocene–Pleistocene succession is marked by a shallow discordance between lower, southward-dipping reflectors and overlying more horizontal reflectors (Taylor, Huchon, Klaus, et al., 1999). Beneath this, the southerly part of the downflexed northerly rift margin is unconformably underlain by an inferred Paleogene ophiolitic unit, whereas the outer rift margin is underlain by Miocene sediments correlated with the Trobriand forearc (Taylor, Huchon, Klaus, et al., 1999). The southern margin of the Woodlark rift is delineated by the Moresby Detachment fault, which dips at 25°–30° to the north-northeast, away from the southern margin of the rift, represented by the Moresby Seamount. Numerous north-south, normal and oblique faults imaged on the Moresby Seamount are consistent with regional north-south extension, as deduced from earthquake fault plan solutions (Abers, 1991; Abers et al., 1997; Mutter et al., 1996; Hegler et al., 1995) and Global Positioning System (GPS) measurements (Tregoning et al., 1998). Drilling during Leg 180 confirmed that the Mo-

resby Seamount is composed of continental crust, rather than being a typical igneous seamount, confirming earlier dredge results from the northeastern flank of this structure, which produced clasts including psammite, phyllite, pelite, greenschist, metagabro, and microgranite (Binns et al., 1990).

North of the Woodlark rift, the Woodlark Rise, part of the Trobriand forearc, is interspersed with several volcanic islands (e.g., Woodlark Island) and seamounts (e.g., Egum atoll), beyond which lies the Trobriand Trough, interpreted as an active south-dipping subduction zone related to the Trobriand arc; farther north again is the Solomon Sea, which is floored by oceanic crust (Davies et al., 1987; Honza et al., 1987).

The Woodlark rift passes northwestward into a large region termed the Cape Vogel Basin as a whole. In detail, the Cape Vogel Basin includes onshore Neogene basins in Papua New Guinea and an adjacent offshore area dominated by terrigenous clastic sediments derived from on shore. Farther offshore there is a large carbonate platform, the "Trobriand Platform," which is studded with coral reefs, atolls, and islands and interspersed with submarine channels.

ANALYTICAL METHODS: SAMPLE PREPARATION

In the majority of Leg 180 samples, it was clear that the main lithology is relatively barren of organic matter. For these, visible fragments of organic matter were handpicked, generally being extracted with a pair of tweezers. For these samples, the abundance of organic matter in the block examined is much greater than that for the average of the sample. With samples containing coal or abundant dispersed organic matter, part of the sample was crushed.

The handpicked or crushed samples were dried in a vacuum oven at normal pressure. A temperature of ~120°C was used in order to stabilize any swelling clays that were present and to minimize the problems associated with low-rank vitrinite that has a high moisture content.

Polished blocks were prepared by mounting the grains of the dried sample in polyester resin (ASTIC) to form "whole-rock" preparations. However, as noted, a high proportion had been handpicked so that they represented whole-rock mounts of selected material. Setting properties of the samples were generally good, with mounting problems being restricted to small number of highly pyritic samples. Normal grinding (silicon carbide papers) and polishing techniques (chromium sesquioxide [GNM grade], followed by magnesium oxide [grade Maglite D/E]) were used for the resin-mounted blocks.

Oil and oil drops are easier to identify in whole-rock mounts, but these proved to be rare overall. Additionally, within whole-rock mounts, identification of organic matter types is more certain because grain outlines and polishing relief are easier to detect. For low-rank vitrinite, use of whole-rock preparations allows observation of textural features free of the effects of demineralization. Organic matter assemblages can only be determined in whole-rock preparations.

Examination of samples in fluorescence mode permits the detection of liptinite macerals and discrimination of suberinite and fluorescing vitrinite. Fluorescence mode was available for making observations on the fields used for vitrinite reflectance measurements, and only small

changes are required to change from fluorescence mode to reflected white light mode to use the photometer.

MEASUREMENT OF REFLECTANCE

Reflectance measurements were made in accordance with AS 2486 using a Leitz MPV 1.1 photometer mounted on a Leitz Orthoplan microscope. The objective used for reflectance measurements was a 50× NPL oil-immersion lens. Synthetic spinel ($R = 0.416\%$) and garnets ($R = 0.817\%$ and 1.76%) were used to calibrate the photometer. The low reflectances of most samples meant that the spinel was generally the primary standard used.

Each reflectance measurement reported is the average of two measurements of the maximum reflectance for the field (back-projected area of the spot size in the field of view on the sample is a rectangle approximately $0.001 \text{ mm} \times 0.002 \text{ mm}$), the two measurements being separated by rotation of the stage by 180° . Stage rotation gives a measure of the local flatness of the polished surface. A minimum of 25 fields were measured on every sample where sufficient vitrinite was present. Where 25 fields were measured, the mean quoted is effectively the average of 50 measurements of vitrinite reflectance.

MEASUREMENT OF ORGANIC MATTER ABUNDANCE

Maceral percentages and bitumen, oil, and oil-drop abundances were determined by visual estimate during linear traverses. This method is more reliable than the point-count technique where the abundance of these components is less than $\sim 10\%$. The maceral classification used is given in Table T1. Other descriptions of maceral classifications can be found in Standards Association of Australia (SAA) (1981), International Committee for Coal Petrology (ICCP) (1971, 1994, 1997), and in Taylor et al., (1998). Of these, only the SAA system and that used here combine the vitrinite and huminite macerals into a single group. However, the classification used here retains those terms within the huminite group that are essentially textural and are related to the extent of gelification. Gelification is due either to processes associated with peat formation or subsequent compaction following burial. Table T2 summarizes the cutoff values used to describe maceral abundance for dispersed organic matter (DOM) and coal as well as for the abundance of rock types and minerals, such as pyrite and glauconite.

Observations were also made on mineral matter fluorescence. Apart from a small number of minerals, such as dolomite and zircon, that fluoresce due to the presence of trace elements, most fluorescence from minerals is due to the presence of small amounts of dispersed and adsorbed bitumens. At low levels of maturation, mineral fluorescence is generally weak and becomes stronger within the oil window. For marine rocks, fluorescence intensity tends to decrease markedly close to the oil thermal limit but persists into the wet gas window in source rocks of terrestrial origin. A patchy distribution of mineral fluorescence is also characteristic of the more mature source rocks that contain organic matter that is terrestrial in origin. Weak to absent mineral fluorescence is generally an indication that a sediment unit is supermature ($R_o > 3.0\%$) but is also characteristic of red-bed units where iron oxides

T1. Maceral groups, subgroups, macerals, and submacerals, p. 18

T2. Maceral abundance cutoffs, p. 19.

cause quenching of the fluorescence emitted. Observations of the alteration of mineral fluorescence with time of irradiation are also made. Data on alteration are reported only where unusual features are noted.

ASSESSMENT OF MATURATION FROM REFLECTANCE

Although the burial depths of the samples are <700 meters below sea-floor (mbsf) and seafloor temperatures are generally low, it was considered that temperatures may have been sufficiently high to cause increased reflectances because of the observed nonbrittle mode of basin subsidence (e.g., Driscoll and Karner, 1998). Further, it was recognized that variation within some of the types of wood tissue (Kantsler and Cook, 1979; Cook and Kantsler, 1980) could also be an important factor in measuring temperatures. In extreme cases, some types of woody tissue are unsuitable for measurement of vitrinite reflectance as an indication of maturation level. These tissue types include suberinite and the tissues preserved as jet. In practice, the presence of low-reflectance cell walls proved to be an important factor for the present suite of samples.

In addition to the reflectance data, interpretation of maturation levels is supported by the (1) presence of fluorescing liptinite and the fluorescence colors, (2) degree of compaction of woody cell structures, (3) mineral matter fluorescence intensity and color, and (4) the organic facies present.

ORGANIC MATTER ABUNDANCE AND TYPE: OVERALL DISTRIBUTION OF ORGANIC MATTER

It should be noted that hand picking of the samples means that these data overstate the amount of organic matter in the whole cores. Even where hand picking of samples was not undertaken, the most organic-rich layers were selected. A summary of the type of organic matter present is given in the comments column of Table T3.

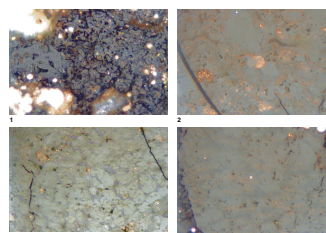
Photomicrographs of the organic matter are shown in Plates P1, P2, P3, P4, P5, P6, P7, P8, P9, P10, P11, P12, P13, and P14. A high proportion of these plates illustrate the woody tissues that form the most abundant type of organic matter. The plates also illustrate the coals found, DOM, and rare oil drops.

The photomicrographs of the samples (all plates) were taken either using white light with the polar removed from the light train or in fluorescence mode using a BG3 excitation filter and the plane slip illuminator. Photographs were taken using lenses with nominal magnifications of 10×, 20×, and 50×. The 10× objective lens is an "air" immersion lens, and the 20× and 50× lenses use oil immersion, but all those used were taken with the 50× lens. Where matching pairs of reflected white light and reflected fluorescence mode are used, the pairs are in registration or are close to being in registration.

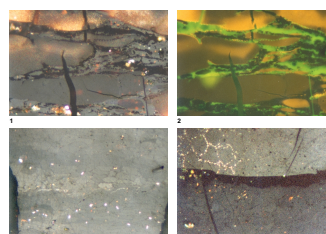
Using microscope techniques, crushed fragments of large pieces of wood tend to report as coal. The distinction between some DOM and coal must also include information relating to the preparation of the samples. However, with the present set of samples where true coals are present, these are finely bedded (in samples from Hole 1109D below 650 mbsf) and are easily distinguished from fragments of drifted logs.

T3. Vitrinite reflectance data, p. 20.

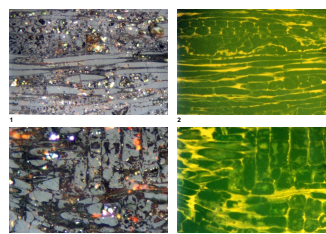
P1. Wood tissues preserved as vitrinite, p. 22.



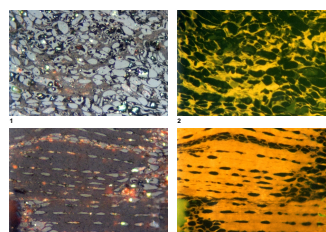
P2. Wood tissues preserved as vitrinite, variable textures, and reflectance, p. 23.



P3. Vitrinite showing fluorescence from cell walls, p. 24.



P4. Variable contribution of cell walls to bulk of vitrinite, p. 25.



Thus, Plates **P9** and **P10** illustrate samples of coal, whereas Plates **P1**, **P2**, **P3**, **P4**, **P5**, and **P6** illustrate fragments of drifted logs. Plate **P11**, figures 3 and 4, illustrate a peat intraclast, and even within a core sample, it is difficult to be certain that larger occurrences of coal do not represent intraclasts. However, it is normally the case that intraclasts show some degree of deformation. Hence, the coals illustrated in Plates **P9** and **P10** are considered autochthonous.

Most DOM occurs as small particles as in Plate **P12**. Most of the small particles of organic matter can be assumed to be allochthonous. However, many of the structures found where DOM is more abundant (as in Plate **P12**) are suggestive of an in situ origin. The telovitrinite in Plate **P13**, figures 3 and 4, are similar to root structures.

Although most samples were deposited in marine conditions, most of the organic matter is terrigenous in origin. The drifted logs could be relatively rare events, and so those samples containing them may not be representative. However, the lithologies that contain larger numbers of particles of DOM are also dominated by higher plant-derived phytoclasts. Phytoplankton are present in some samples but are typically a minor part of the organic matter population.

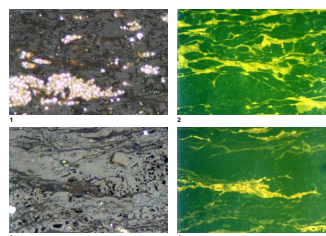
Overall, the organic matter assemblage is dominated by vitrinite (see plates). Liptinite is the second most abundant maceral group. The most common form of liptinite is suberinite, and most of this is associated with the large wood fragments that are dominant in the majority of samples. The coal and shaly coal samples contain a diverse range of liptinite and represent the highest liptinite content other than suberinite. Small amounts of cutinite are present mostly as DOM. Plate **P13**, figures 1 and 2, show well-preserved leaf cuticle, but such good preservation is unusual. Although most of the samples were undoubtedly deposited under marine conditions, liptinite derived from phytoplankton is relatively rare and has been reported as lamalginite. Most of the lamalginite occurs as thin-walled tests.

Inertinite is widely distributed, but most represents fungal tissues preserved as funginite (Plate **P14**, figs. 3, 4). This maceral was previously referred to as sclerotinite, but the members of ICCP, meeting at Wellington in 1987, agreed to the change in terminology. The presence of funginite indicates some decay of the tissues under aerobic conditions. Funginite comes from Basidiomycete and Ascomycete fungi, and these do not survive immersion in water, especially saline water. In two samples, the organic matter consists almost entirely of fusinite and semifusinite. This represents the residues from forest fires. Both of these samples are overlain and underlain by samples that lack fusinite and semifusinite. They appear to represent relatively rare forest fire events. The fusinite and semifusinite in the sample from Hole 1115A shows a high mean reflectance of 3.44%, with a range from 1.38% to 5.24%.

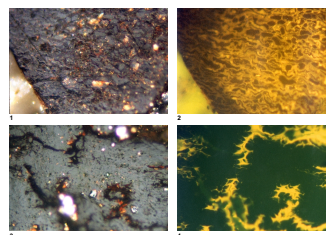
HUMINITE AND VITRINITE

The humic macerals in the samples are dominated by low-reflectance humic materials. In terms of the definitions of ICCP (1971), the low reflectance forms should be referred to huminite. However, this material becomes vitrinite at higher levels of rank, and the use of huminite is considered by many authors to be confusing. Using ICCP terminology, essentially the same component changes from the huminite group to the vitrinite group at a reflectance of 0.5%. The Australian Standard has

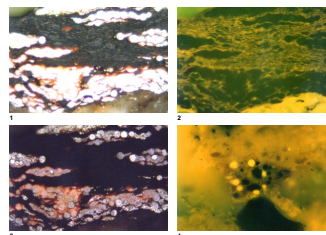
P5. Cell walls transitional to suberinite, p. 26.



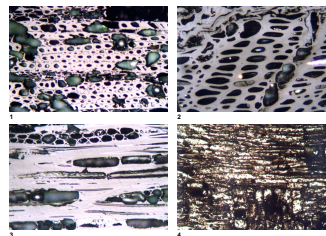
P6. Suberinite and cutinite, p. 27.



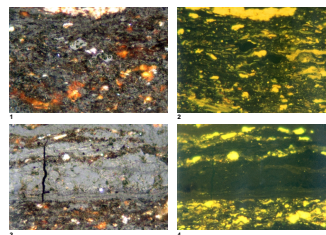
P7. Vitrinite, pyrite, and oil inclusions, p. 28.



P8. Pyrofusinite and pyrite replacement of woods, p. 29.



P9. Coal and shaly coal, p. 30.



combined the two materials within the vitrinite group, and this terminology is the basis of the classification used here (see Table T1).

In the Australian Standard (SAA), the textural differences that are a function of rank (that is, textures can be different for the lower and higher rank forms of vitrinite) are identified and separated at the maceral level. The classifications are identical at group and subgroup levels.

The dominant forms of organic matter present in this sample suite belong to the telovitrinite subgroup. Within this group, textinite, textulminite, and ulminite are all present, and some material is best considered as telocollinite, a term normally restricted to some forms of vitrinite present in higher-rank coals. Discussions of the compaction of structures within vitrinite are given in Taylor et al. (1998) and Teichmüller and Teichmüller (1950).

The Australian Standard builds on the ICCP (1971) classification for low-rank coals. At a general level, this classification proved adequate. However, at a more detailed level it has proved inadequate in relation to woody tissues that show low reflectance and moderate to strong fluorescence, largely from the primary cell walls. In the ICCP (1971) classification, primary fluorescence is considered as coming only from suberinite, the primary cell wall material associated with bark tissues.

However, in the present study, many examples were found of xylem tissues with primary cell walls showing fluorescence as strong or stronger than suberinite in the same sample. These tissue types are illustrated in Plate P3, figures 3 and 4, and Plate P4, figures 1–4. Generally, the fluorescing cell walls have not been counted as liptinite, even though in terms of optical properties, they resemble that maceral group much more closely than vitrinite.

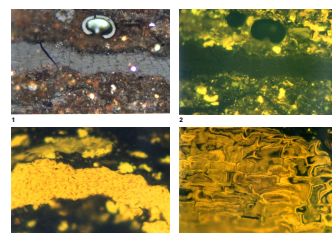
LARGE VITRINITE PHYTOCLASTS

Vitrinite occurring as large phytoclasts is the dominant phase in a high proportion of the organic matter (Table T3). Most of these large phytoclasts show excellent preservation of the cell structures (Plates P1, P2, P3, P4, P5, P6). The textures range from textinite (less common) to textulminite (most common) and ulminite (common). Bark tissue is present, and suberinite is found there in association with phlobaphinite.

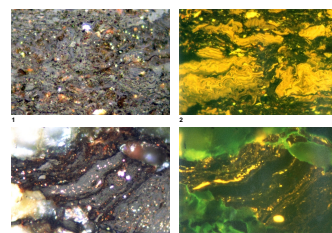
Where distinct cell structures are present, the cell contents almost all have a higher reflectance compared with the cell walls. The ratio of the reflectance of the cell contents to that of the cell walls is typically between 2 and 3 to 1. Thus, most cell contents show reflectances between 0.3% and 0.4% and the cell walls between about 0.08% and 0.18%. Typical cell structures are shown in Plate P1. The contrast between texturally immature vitrinite (Plate P2, figs. 1, 2) and texturally mature vitrinite (Plate P2, figs. 3, 4) is shown in Plate P2.

Plates P3 and P4 illustrate the unusual very low reflecting and strongly fluorescing primary cell wall tissues found in some wood structures. Medullary rays are present in the fields illustrated in Plate P3, and they represent xylem tissues. Such a large reflectance and fluorescence contrast is not normally associated with xylem tissues. Plate P4 illustrates the variable amounts of low-reflecting tissue. The mean reflectance for the field in Plate P4, figure 1, would be evenly weighted between the higher reflecting cell contents and the cell walls. In the field in Plate P4, figure 3, the mean would be heavily weighted toward the low-reflecting cell walls.

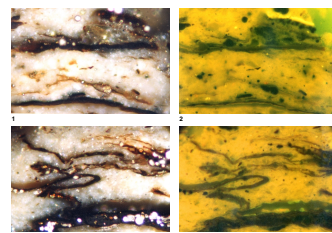
P10. Coal and shaly coal-cork cells and suberinite, p. 31.



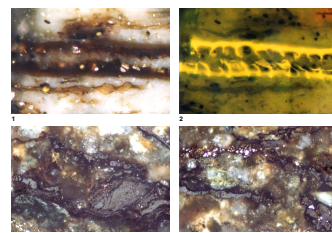
P11. Coal and coal intraclasts, p. 32.



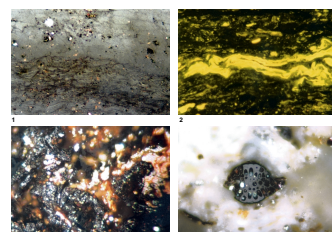
P12. Dispersed organic matter, p. 33.



P13. Dispersed organic matter, p. 34.



P14. Suberinite, fungal tissues, p. 35.



Some of the low-reflectance cell walls are transitional to suberinite. Some of these fields are illustrated in Plate **P5**. Plate **P6** illustrates suberinite tissues and also shows the effects of prolonged irradiation on both the cell walls and cell fillings. Fluorescence intensity is increased on prolonged irradiation, and the reflectance of both the cell walls and contents is lowered. Plate **P6**, figures 3 and 4, illustrate cuticle tissues present on woody tissues. This type of cutinite is similar chemically but differs in tissue associations from the leaf cutinite illustrated in Plate **P13**, figures 1 and 2.

Where cell structures are well defined (as in Plates **P1**, **P3**, **P4**, **P5**), it is possible to selectively measure the reflectance of cell contents and these are considered to be more representative of maturation (coal rank) compared with the values obtained from the cell walls. However, in many fields, similar tissues appear to be present but the cell walls cannot be separated from the cell contents. Plate **P2**, figure 3, shows a tissue with a range from 0.54% to 0.24%. Some of these differences are related to the contrast between cell walls and contents, but at least three major different tissue layers can be distinguished in this field. In the field illustrated by Plate **P7**, figure 4, and Plate **P8**, some cell outlines are shown by pyrite inclusions but no major differences can be seen between cell contents and cell walls. However, the lower layer shows a reflectance of 0.26% and the upper layer 0.48%. Although the vitrinite in Plate **P2**, figure 4, is very low in rank, the textures are essentially those of telocollinite, a maceral normally considered as being restricted to the bituminous rank range.

Overall, it is clear that tissue type exerts a major influence on the mean reflectances obtained. Where cell walls can be distinguished, it is possible to minimize this variation by restricting measurements to the cell contents, as these proved to show less variation. However, for many samples, low-reflecting tissues are present that do not show cell structures. In a small proportion of samples, these low-reflecting homogeneous tissues are the only population present. Thus, it was not possible to eliminate the effects of tissue type on the reflectances obtained.

FUSINITE AND SEMIFUSINITE ASSEMBLAGES

In two samples, the organic matter is dominated by fusinite and semifusinite and vitrinite is not present. The inertinite represents residues from forest fires, and the absence of coexisting vitrinite may indicate that an extensive charring episode occurred. Both these samples are overlain and underlain by samples that lack fusinite and semifusinite and show vitrinite reflectances similar to those of other samples. From this, it can be inferred that charring took place in the source provenance for the wood and that charring was restricted to a small time interval. Thus, the inertinite appears to represent material produced in relatively rare forest fire events.

The fusinite and semifusinite in the sample from Hole 1115A show a high mean reflectance of 3.44%, with a range from 1.38% to 5.24%. These values are unusually high for fusinite in low-rank sequences, and are high even for commercial charcoals. The fusinite and semifusinite in Hole 1118C show a lower mean reflectance of 1.00%, with a range from 0.80% to 1.30%.

DISPERSED ORGANIC MATTER ASSEMBLAGES

DOM is the dominant form of organic matter in a number of the samples (Plate P12). Most of the material considered as DOM in this report comprises fragments ranging up to about 0.3 mm, too small to be handpicked. In the case of the present suite, the DOM has vitrinite as the major component. The DOM suites are typically vitrinite > liptinite > inertinite. The vitrinite in DOM generally consists of small particles of detrovitrinite. However, some occurrences of telovitrinite are present, as illustrated in Plate P13, figures 3 and 4. In these fields, the telovitrinite appears to represent root tissues, possibly from a root horizon of mangrove or *Nypa*-type vegetation.

Most of the liptinite consists of phytoplankton preserved as lamalginite. Tests are thin walled, and this maceral is generally rare. Some sporinite is also present. Cutinite is prominent in a restricted number of horizons. A high proportion of the cutinite is weakly fluorescing, as illustrated in Plate P13, figures 1–4. This could reflect derivation from tropical rainforests where thickened cuticles are relatively rare but could also be due to early diagenetic alteration. The cutinite illustrated in Plate P13, figures 1 and 2, is leaf derived and shows the characteristic serrate inner margins. Cutinite is relatively rare in marine sediment, and even within nonmarine sections is much less common in DOM compared with associated coals. The presence of well-preserved cutinite may indicate proximity to the source areas for the plant matter.

COALS AND SHALY COALS

Coals and shaly coals are present in a number of samples from Hole 1109D in the deeper part of the section. These appear to be hyp-autochthonous in origin. However, it is possible that the samples are themselves part of large peat intraclasts, but this does not appear to be likely. The coals and shaly coals are typical of Tertiary peats and show affinities to the Miocene coals that are widely distributed through Papua New Guinea and southeast Asia. Liptinite is abundant to major within these coals, but they are dominated by vitrinite. Inertinite is present as small amounts of funginite (sclerotinite).

The vitrinite occurs both as telovitrinite and detrovitrinite (Plate P9, figs. 1–4; Plate P10, figs. 1–4; Plate P14, fig. 2). Detrovitrinite is more widely distributed than telovitrinite, but the large size of the telovitrinite phytoclasts means that it is more abundant overall within the coals. No major differences in reflectances between detrovitrinite and telovitrinite were found (cf. Plate P9, fig. 1; Plate P9, fig. 3). This is probably because most of the detrovitrinite represents isolated cell fillings from woody tissue, and this is the component used in vitrinite reflectance measurements made on the telovitrinite.

A range of liptinite macerals is present, sporinite, resinite, suberinite, cutinite, and liptodetrinite. Resinite and resin-related liptodetrinite are generally the most abundant. However, the larger liptinite phyterals are more prominent features, for example, the strongly fluorescing suberinite seen in Plate P10, figure 4. Inertinite within the coals is effectively confined to funginite (sclerotinite). Plate P10, figure 1, illustrates a large teleutospore seen in transverse section. Plate P9, figure 1, also contains some less easily distinguished funginite.

Plate P11, figures 3 and 4, illustrate a small peat intraclast occurring within a sandy sediment. The coal type is similar overall to that illus-

trated in Plate P9, figures 1 and 2. In this case, the intraclast origin is clear from the discordant nature of the bedding. However, peat clasts tend to be platy, and it is possible that the other occurrences of coal and shaly coal are also intraclasts, as the contact with the surrounding lithologies was not seen.

FUNGAL TISSUES

Fungal tissues are present within some samples, most commonly representing teleutospores (Plate P10, fig. 1) and sclerotia (Plate P14, fig. 4). Teleutospores represent the normal "spore" forms used by fungi for their dispersal. Sclerotia are fungal resting spores and are formed during times of stress as a result of high temperatures and desiccation. Fungal hyphae are present (Plate P14, fig. 3), and although rare, they tend to be widely distributed through woody tissue. The hyphae represent the main growth parts of fungal colonies but commonly show reflectances very close to those of vitrinite and cannot always be distinguished from vitrinite. Small amounts of fungal fruiting bodies (stromata) were also found.

The presence of fungal tissues is significant in relation to the setting in which the organic matter was generated. It suggests that normal near-surface rotting of wood occurred prior to its being washed away and included within the marine sediments.

EVIDENCE OF HYDROCARBONS

Oil odor had been reported from some of the cores, and care was taken to examine all samples for the presence of oil drops. The only examples were found in Hole 1115C at 514.72 mbsf. These are clearly indigenous oil drops. Some possible occurrences of oily material were found but were considered to represent additives similar to pipe dope. It is possible that the moderate-temperature drying has tended to evaporate oils. However, the higher boiling fractions would have been left, and these are normally the more strongly fluorescing components. It is therefore concluded that oil is not prominent within the sections drilled.

VITRINITE REFLECTANCE

Vitrinite reflectance measurements were obtained for almost all of the samples. However, for a high proportion of samples, the readings come from a small number of phytoclasts, and in some cases, from only a single plant entity. It is clear that plant and tissue types are the main control over the values obtained rather than thermal history. The degree of compaction of the vitrinite may be a better indication of cover and heating than vitrinite reflectance for this suite of samples. The variation in reflectance of various tissue types precludes correlating vitrinite reflectance with thermal regimes, primarily because measured borehole temperatures and temperatures calculated from the observed sediment thermal conductivities and range in basement heat flow (Fig. F2) are too low to have caused a marked affect on vitrinite reflectance. In contrast, where reflectances exceed ~0.45%, these values probably result from maturation effects. However, texturally mature vitrinite can de-

velop either due to compaction associated with the early stages of physico-chemical coalification or to gelification in the peat stage. The presence of relatively massive structures at moderate to shallow depths (e.g., Plate P1, figs. 3, 4) suggests that gelification within the peat stage must have been extensive. It is, however, possible that the more gelified tissues were more likely to be preserved after transport and sinking through the water column. In particular, the less massive tissues may have tended to float rather than sink to be included within the sediments.

No clear trend in vitrinite reflectance exists within or among individual well sections. Even textural features do not show any marked trends. For example, Plate P2, figure 1, illustrates texturally immature vitrinite but is from one of the deeper samples in the suite. There is, however, a weak tendency for the more open cell structures such as those illustrated in Plate P3, to occur at shallow to moderate depths. The lack of trends within vitrinite reflectance suggest that formation temperatures even in the deeper samples have not exceeded ~50°C. Temperatures above this level are required before vitrinite reflectance shows any marked increase from the levels associated with woody material preserved within peats.

ORIGIN OF THE ORGANIC MATTER

The organic matter is dominantly vitrinite. A small proportion of the vitrinite may have grown in a marginal marine setting, but most appears to have grown inland. The coal and shaly coals show assemblages typical of ombrogenous settings, although the abundance of minerals suggests a low-moor inland setting rather than a high moor. The presence of fungal tissues suggests that wood-rotting fungae were able to live in the areas that were the source of the woody tissues. This is consistent with an origin from an inland rather than a marginal marine setting. However, most of the wood tissues are relatively intact, and the extent of fungal attack appears, overall, to have been small. The preservation of the wood structures within the large isolated wood fragments is generally better than in the coals and shaly coals.

Some coaly intraclasts are undoubtedly present (Plate P11, figs. 3, 4). The root tissues, such as those figured in Plate P13, figures 3 and 4, suggest that some in situ plant tissue are present. The preservation of some of the cutinite is also indicative of minimal transport for at least some of the organic matter.

Fusinite and semifusinite are restricted to two samples. Both of these components tend to float, so lack of these macerals could be due to a low tendency for sinking in the water column. However, it is also possible that the horizons that contain these two macerals represent relatively rare forest fire events in the source areas.

Marine liptinite is a relatively minor component of the organic matter assemblages. The general paucity of phytoplankton may suggest relatively low productivities in the overlying water columns.

CONCLUSIONS

All of the samples contain some organic matter, and for most it was possible to measure at least 25 fields of vitrinite for reflectance. A high proportion of the vitrinite appears to represent drifted logs. Within

most of these, tissue preservation is excellent. Variations in vitrinite reflectance relate mainly to tissue type. It is also possible that the species of wood preserved has an influence on the values obtained. To minimize the effects of tissue type, measurements were largely restricted to the cell contents in most cases. Some vitrinite is preserved in a form similar to telocollinite, and this form was also found to show marked reflectance variations that are also presumed to relate to tissue or wood type.

Vitrinite preserved as smaller particles of dispersed organic matter has reflectances generally similar to those obtained on the larger particles. This is presumed to be because the smaller particles selectively represent the cell filling, corpocollinite.

Liptinite is generally a minor component in the organic matter assemblage. Marine phytoplankton preserved as lamalginite represents the most widely distributed form of liptinite, but lamalginite is a minor component. Abundant foraminiferal tests are present in many of the samples, but this abundance of fossil remains is not matched by an abundance of marine-sourced organic matter. Terrestrially sourced liptinite is also present but is most abundant in samples that are either terrestrial in origin or represent intraclasts of terrestrial origin.

Samples of coal and shaly coal are present in the deeper part of the Hole 1109D section. These may represent hypautochthonous peats. Two samples are dominated by fusinite and semifusinite. These may represent forest fire episodes in the source areas for the organic matter. Material interpreted as air-fall tuffs is abundant in a high proportion of the samples, but its presence cannot be correlated with the presence of forest fire charcoal. Variation of vitrinite reflectance is not systematic with either depth or location, and it appears that the formation temperatures of 10°–80°C, and/or the time over which the organic material has been exposed to these temperatures, have not been sufficient to cause an increase in vitrinite reflectance levels. Vitrinite texture is relatively sensitive to the depth of cover, and it is normally possible to detect systematic variation in the ratio of textinite to ulminite in the top 500 to 700 m of the section. This did not prove possible in the present case. It seems unlikely that this is due to cover loss, and it is more probable that it has been caused by selective preservation of the more strongly gelified tissues. Thus, the relative lack of textinite may be due to the depositional setting rather than to the extent of gelification that has occurred either as a process during peat formation or during the early stages of compaction.

ACKNOWLEDGMENTS

We acknowledge critical reviews of the manuscript by Michael Underwood, Brian Taylor, and an anonymous reviewer. This research used samples and/or data provided by the Ocean Drilling Program (ODP). The ODP is sponsored by the U.S. National Science Foundation (NSF) and participating countries under management of Joint Oceanographic Institutions (JOI), Inc. Funding for this research was provided by JOI/USSSP contract USSSP 180-F000907; Lamont-Doherty Earth Observatory publication #6346.

REFERENCES

- Abers, G.A., 1991. Possible seismogenic shallow-dipping normal faults in the Woodlark-D'Entrecasteaux extensional province, Papua New Guinea. *Geology*, 19:1205–1208.
- Abers, G.A., Mutter, C.Z., and Fang, J., 1997. Shallow dips of normal faults during rapid extension: earthquakes in the Woodlark-D'Entrecasteaux rift system, Papua New Guinea. *J. Geophys. Res.*, 102:15301–15317.
- Benes, V., Scott, S.D., and Binns, R.A., 1994. Tectonics of rift propagation into a continental margin: western Woodlark Basin, Papua New Guinea. *J. Geophys. Res.*, 99:4439–4455.
- Binns, R.A., Scott, S.D., Wheller, G.E., and Benes, V., 1990. Report on the SUPACLARK cruise, Woodlark Basin, Papua New Guinea, April 8–28 1990, RV *Akademik Mstislav Keldysh*. CSIRO Rep. 176R.
- Binns, R.A., and Whitford, D.J., 1987. Volcanic rocks from the western Woodlark Basin, Papua New Guinea. *Proc. Pac. Rim Congr.*, 87:525–534.
- Cook, A.C., and Kantsler, A.J., 1980. The maturation history of the epicontinental basins of Western Australia. *Tech. Bull.—U.N. Econ. Soc. Comm. Asia Pac., Comm. Co-ord. Jt. Prospect. Miner. Resour. South Pac. Offshore Areas*, 3:171–195.
- Davies, H.L., Honza, E., Tiffin, D.L., Lock, J., Okuda, Y., Keene, J.B., Murakami, F., and Kisimoto, K., 1987. Regional setting and structure of the western Solomon Sea. *Geo-Mar. Lett.*, 7:153–160.
- Driscoll, N.W., and Karner, G.D., 1998. Lower crustal extension along the Northern Carnarvon Basin, Australia: evidence for an eastward dipping detachment. *J. Geophys. Res.*, 103:4975–4992.
- Goodliffe, A., Taylor, B., Hey, R., and Martinez, F., 1993. Seismic images of continental breakup in the Woodlark Basin, Papua New Guinea. *Eos*, 74:606.
- Goodliffe, A., Taylor, B., Martinez, F., Hey, R., Maeda, K., and Ohno, K., 1997. Synchronous reorientation of the Woodlark Basin spreading center. *Earth Planet. Sci. Letters*, 146:233–242.
- Honza, E., Davies, H.L., Keene, J.B., and Tiffin, D.L., 1987. Plate boundaries and evolution of the Solomon Sea region. *Geo-Mar. Lett.*, 7:161–168.
- International Committee for Coal Petrology, 1971. *International Handbook of Coal Petrology, Supplement to the 2nd Edition*: Paris (Cent. Nat. Rech. Sci.).
- , 1994. *Vitrinite Classification*. Rev. approved at Oviedo Mtg. of ICCP.
- , 1997. Minutes of Commission I. Annu. Int. Mtg., *ICCP Newsletter*.
- Kantsler, A.J., and Cook, A.C., 1979. Maturation patterns in the Perth Basin. *APEA. J.*, 19:94–107.
- Murchison, D.G., Cook, A.C., and Raymond, A.C., 1985. Optical properties of organic matter in relation to thermal gradients and structural deformation. In Eglington, G., Curtis, C.D., McKenzie, D.P., and Murchison, D.G. (Eds.), *Geochemistry of Buried Sediments*. Philos. Trans. R. Soc. Lond., Ser. A, 315:157–199.
- Mutter, J.C., Mutter, C.Z., and Fang, J., 1996. Analogies to oceanic behavior in the continental breakup of the western Woodlark Basin. *Nature*, 380:333–336.
- Robertson, A.H.F., Awadallah, S., Gerbaudo, S., Lackschewitz, K.S., Monteleone, B.D., Sharp, T.R., and other members of the Shipboard Scientific Party, 2001. Evolution of the Miocene–Recent Woodlark rift basin, SW Pacific, inferred from sediments drilled during Ocean Drilling Program Leg 180. In Wilson, R.C.L., Whitmarsh, R.B., Taylor, B., and Froitzheim, N. (Eds.), *Non-Volcanic Rifting of Continental Margins: A Comparison of Evidence from Land and Sea*, Spec. Publ.—Geol. Soc. London, 187:335–372.
- Standards Association of Australia, 1981. *Methods for Microscopical Determination of Reflectance of Coal Macerals: AS 2486*. North Sydney (Stand. Assoc. Aust.).
- Taylor, B., Goodliffe, A.M., and Martinez, F., 1999. How continents break up: insights from Papua New Guinea. *J. Geophys. Res.*, 104:7497–7512.

- Taylor, B., Huchon, P., Klaus, A., et al., 1999. *Proc. ODP, Init. Repts.*, 180 [CD-ROM]. Available from: Ocean Drilling Program, Texas A&M University, College Station, TX 77845-9547, U.S.A.
- Taylor G.H., Teichmüller, M., Davis, A., Diessel, C.F.K., Littke, R., and Robert, P., 1998. *Organic Petrology*: Berlin (Gebrüder Borntraeger).
- Teichmüller, M., and Teichmüller, R., 1950. Das Inkohlungsbild des niedersächsischen Wealdenbeckens. *Z. Dtsch. Geol. Ges.*, 100:489–517.
- Tregoning, P., Lambeck, K., Stolz, A., Morgan, P., McClusky, S., Van de Beek, P., McQueen, H., Jackson, R., Little, R., Laing, A., and Murphy, B., 1998. Estimation of current plate motions in Papua New Guinea from Global Positioning Systems observations. *J. Geophys. Res.*, 103:12181–12203.
- Weissel, J.K., Taylor B., and Karner, G.D., 1982. The opening of the Woodlark Basin, subduction of the Woodlark spreading system and the evolution of northern Melanesia since mid-Pliocene time. *Tectonophysics*, 87:253–277.

Figure F1. Shaded relief bathymetric map showing locations of Leg 180 drill sites near Moresby Seamount, Papua New Guinea, also showing the locations of multichannel seismic tracks. Contour interval is 200 m (thicker contours are labeled every kilometer).

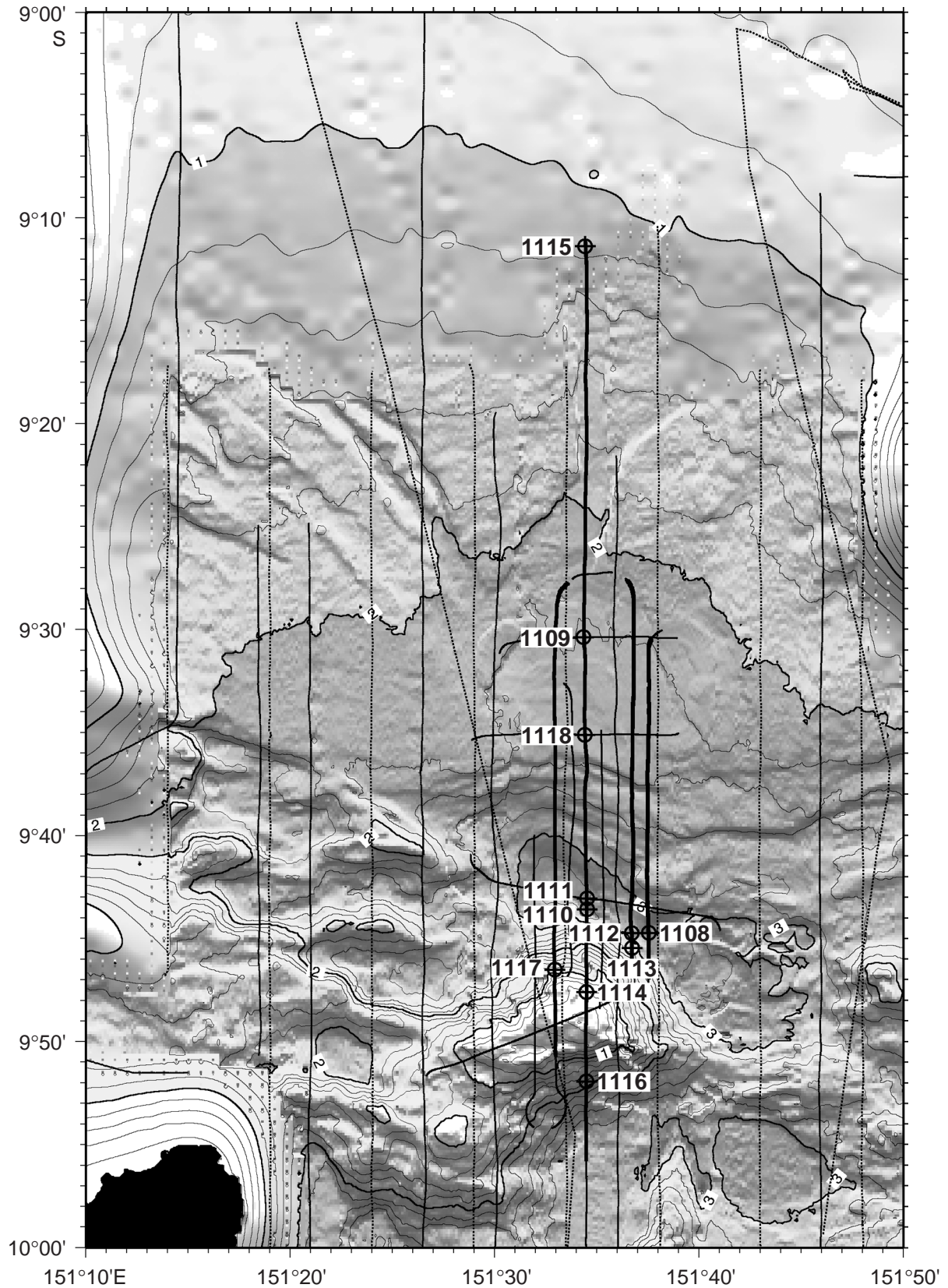


Figure F2. Estimates of thermal gradient and maximum temperatures assuming end-member values of basal heat flux (28 and 100 mW/m²) and using the measured sediment thermal conductivities obtained during Leg 180 drilling for a range of sites. Maximum calculated sediment temperatures are predicted to be ~85°C—observed temperatures are significantly less than this value. Measured maximum temperatures range from 28° and 31°C for Sites 1115 and 1109, respectively. Sites 1108 and 1118 have maximum temperature gradients of 100° and 60°C km⁻¹. Such sediment temperatures are ineffective in affecting vitrinite reflectance.

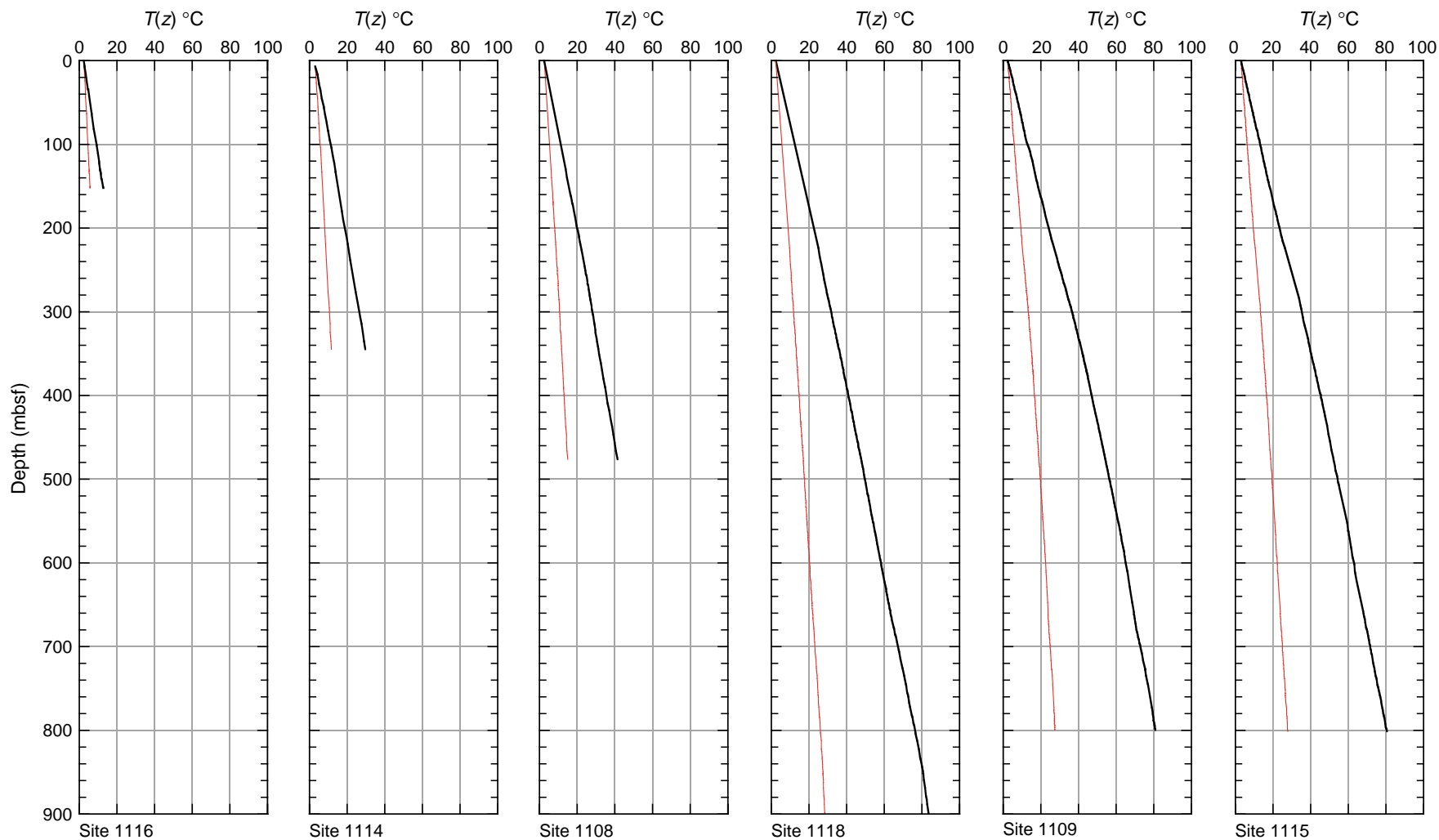


Table T1. Maceral groups, subgroups, macerals, and submacerals.

Maceral group	Maceral subgroup	Maceral	Submaceral
Vitrinite	Telovitrinite	Textinite	Textinite A and B
		Texto-ulminite	Telinite
		Eu-ulminite	
	Detrovitrinite	Telocollinite	Collinite
		Arrinite	
		Densinite	
		Desmocollinite	
		Corpogelinite	
		Porigelinite	
		Eugelinite	
Gelovitrinite	Fusinite		
	Semifusinite		
Teloinertinite			
Inertinite	Detroinertinite	Sclerotinite	
		Inertodetrinite	
		Micrinite	
		Sporinite	
		Cutinite	
		Suberinite	
		Resinite	
Liptinite		Fluorinite	
		Liptodetrinite	
		Alginite	Telalginite Lamalginite
		Bituminite	
		Exsudatinite	

Table T2. Cut-off values used to describe maceral abundance.

Category	Percentage (by volume)
Absent	0.0
Rare	<0.1
Sparse	0.1–0.4
Common	0.5–1.9
Abundant	2.0–9.9
Major	10.0–50.0
Dominant	50.1–100

Table T3. Summary of vitrinite reflectance data for samples. (See table notes. Continued on next page.)

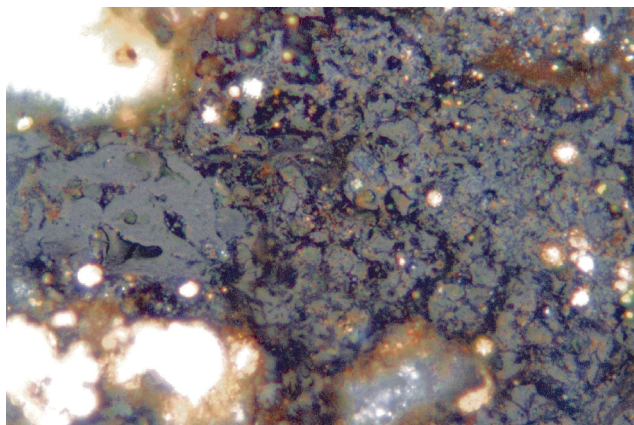
KK#	Hole	Depth (mbsf)	R_v max	Range R_v		N	Comments
				Low	High		
T5799	1108B	216.82	0.38	0.27	0.49	27	TV probably large piece of wood, suberinite present
T5800	1108B	235.77	—	—	—	—	Barren
T5801	1108B	306.35	0.34	0.25	0.46	26	Coalified wood, massive
T5802	1108B	315.79	0.37	0.27	0.50	27	Large pieces of coalified wood
T5803	1108B	324.40	0.39	0.31	0.50	29	Coalified wood fragments
T5804	1108B	333.28	0.41	0.30	0.53	26	Coalified wood fragments
T5805	1109C	180.23	0.36	0.24	0.58	9	Bryozoan fragments, DOM rare
T5806	1109C	217.32	0.35	0.24	0.45	28	Abundant "coal," probably drifted logs
T5807	1109C	296.96	0.36	0.28	0.46	11	Bryozoan fragments, DOM rare
T5808	1109D	379.99	0.23	0.20	0.25	15	Abundant "coal," probably drifted wood
T5809	1109D	387.86	0.36	0.28	0.40	28	Coalified drifted wood
T5810	1109D	427.06	0.28	0.20	0.50	12	Coalified drifted wood
T5811	1109D	447.72	0.34	0.24	0.46	6	Coalified drifted wood
T5812	1109D	533.81	0.35	0.16	0.53	20	Large coalified wood fragments
T5813	1109D	543.38	0.36	0.24	0.46	26	DOM sparse
T5814	1109D	551.24	0.31	0.21	0.48	26	DOM sparse
T5815	1109D	591.05	0.24	0.20	0.33	25	Strong fluorescence from coalified wood
T5816	1109D	672.57	0.29	0.22	0.41	27	DOM sparse
T5817	1109D	688.21	0.40	0.24	0.54	25	Suberinite present in drifted wood
T5818	1109D	696.89	0.28	0.22	0.35	29	Coal representing a peat bed
T5819	1109D	703.23	0.39	0.28	0.49	25	Coal representing a peat bed
T5820	1109D	706.56	0.30	0.22	0.40	25	Probably drifted wood but similar to coals
T5821	1114A	55.42	0.31	0.21	0.42	29	Drifted wood, coalified
T5822	1114A	64.72	0.32	0.24	0.44	27	Coalified drifted wood
T5823	1114A	76.20	0.32	0.21	0.42	27	Rare glauconite
T5824	1114A	85.05	0.33	0.22	0.43	27	DOM abundant, rare drifted wood
T5825	1114A	123.29					Barren, carbonate cement
T5826	1114A	133.23	0.30	0.24	0.36	26	Drifted wood with some bark
T5827	1115A	3.72	0.17	0.10	0.27	25	Wood but fluorescence similar to suberinite
T5828	1115B	241.48	0.22	0.12	0.53	21	Bark and wood tissues
T5829	1115B	272.84	(3.44)				Fusinite and semifusinite representing charred wood
T5830	1115B	291.07	0.25	0.17	0.40	26	Wood structures well preserved
T5852	1116A	24.68	0.30	0.18	0.40	15	Large wood fragments, DOM common
T5831	1115C	303.88	0.32	0.18	0.47	20	Air-fall tuffs, DOM rare
T5832	1115C	304.21	0.33	0.23	0.43	26	Air-fall tuffs, DOM rare
T5833	1115C	323.12	0.32	0.23	0.40	26	Coalified wood, DOM rare
T5834	1115C	325.62	0.27	0.19	0.44	26	Large coalified wood fragments, air-fall tuffs
T5835	1115C	392.67	0.30	0.22	0.41	26	Large coalified wood fragments, DOM rare
T5836	1115C	401.04	0.34	0.23	0.45	27	Some wood, variable coalification
T5837	1115C	411.60	0.33	0.22	0.41	27	Some wood, variable coalification
T5938	1115C	422.84	0.33	0.27	0.41	14	Large drifted coalified wood fragments
T5839	1115C	448.10	0.35	0.22	0.45	16	Fungal sclerotia present, tuffaceous
T5840	1115C	489.50	0.29	0.16	0.49	25	Pyritized wood
T5841	1115C	505.71	0.24	0.12	0.42	26	Low reflecting wood tissue dominant
T5842	1115C	514.24	0.29	0.20	0.39	27	Leaf tissues present
T5843	1115C	562.86	0.29	0.20	0.38	28	Large drifted coalified wood fragments
T5844	1115C	563.60	0.29	0.22	0.40	27	Drifted coalified logs within sediment
T5845	1115C	690.30	0.31	0.23	0.43	25	Oil drops present, DOM common
T5846	1115C	708.03	0.31	0.23	0.39	28	DOM abundant. TV less common
T5847	1115C	722.26	0.33	0.26	0.43	30	Some more highly reflecting TV
T5848	1115C	737.63	0.34	0.23	0.44	29	Some resinous woods
T5849	1115C	746.03	0.33	0.28	0.48	28	DOM abundant, air-fall tuffs
T5850	1115C	757.19	0.33	0.23	0.43	27	DOM common, DV>TV
T5851	1115C	776.48	0.35	0.24	0.46	27	DOM abundant, air-fall tuff present
T5857	1118A	286.47	0.26	0.16	0.35	25	Immature textinite
T5858	1118A	485.79	0.27	0.17	0.43	17	DOM rare, air-fall tuffs
T5859	1118A	580.69	0.27	0.21	0.34	19	DOM abundant, DV dominantly ?bark derived, fresh crystal tuffs
T5860	1118A	624.68	0.33	0.20	0.44	26	Xylem-derived TV, air-fall tuffs
T5861	1118A	725.88	(1.00)				Fusinite and semifusinite from charred wood fragments
T5862	1118A	735.65	0.28	0.20	0.35	25	Some bark tissue; pyritized foraminifers, tuffs
T5863	1118A	744.23	0.36	0.24	0.54	26	Ulminite, some with higher reflectance tissues
T5864	1118A	763.26	0.25	0.15	0.46	20	Coalified wood, some low reflecting TV but with telocollinite texture
T5865	1118A	765.56	0.28	0.17	0.46	28	DOM abundant, bark tissues dominant, crystal tuffs
T5866	1118A	774.45	0.32	0.22	0.50	27	DOM abundant, some texto-ulminite, air-fall tuffs

Table T3 (continued).

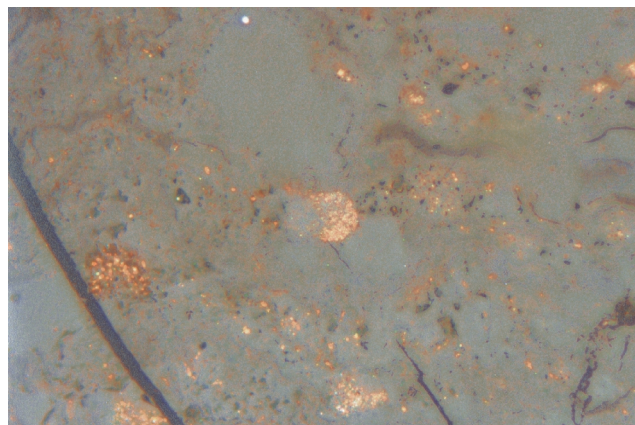
KK#	Hole	Depth (mbsf)	R_v max	Range R_v		N	Comments
				Low	High		
T5867	1118A	811.15	0.19	0.14	0.37	14	Small part hand-picked sample, vitrinite porous, possible cellulose present
T5868	1118A	827.36	0.26	0.20	0.34	28	DOM major, eu-ulminite dominant, air-fall tuffs
T5869	1118A	851.30	0.21	0.19	0.23	3	DOM rare, air-fall tuffs

Notes: R_v = vitrinite reflectance. DOM = dispersed organic matter. N = number of analyses. KK# = internal sample identification number. TV = telovitrinite, DV = detrovitrinite.

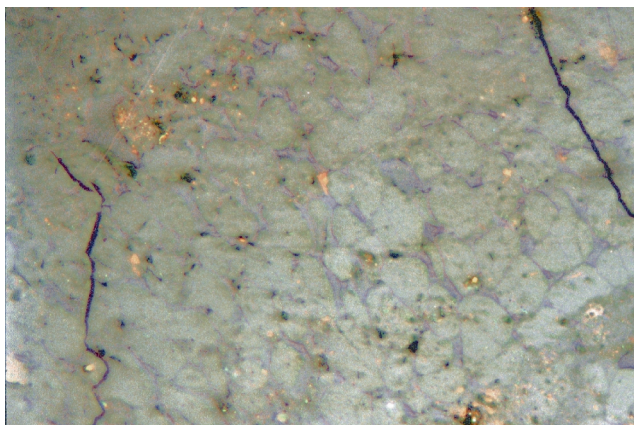
Plate P1. Woody tissues preserved as vitrinite. 1. T5945; Hole 1109C; 217.32 mbsf. Most of the gray reflecting material probably represents cell contents, and some suberinite and resinite are also present but are of extremely low reflectance. No major differences are obvious associated with the cell structures. The wood represents a phytoclast deposited in a marine setting. This type of vitrinite shows reflectances in the middle part of the range and is the most appropriate for use in rank assessments (reflected light; field width = 0.22 mm; vitrinite reflectance = 0.33%). 2. T5945; Hole 1116A; 102.14 mbsf. Cell contents have been humified and show slightly higher reflectances compared with the cell walls. Some small voids are present within some cell lumens, resulting in the presence of bright internal reflectances. These occurrences are referable to porigelinite. The ICCP (1971) terminology would include the cell contents in collinite, whereas the SAA system would place it within telovitrinite. Small differences are present in reflectance between the cell contents and the cell walls and neither shows distinctive fluorescence, so the fluorescence-mode image is not included (reflected light; field width = 0.22 mm; telovitrinite reflectance = 0.51%–0.46%). 3. T5855; Hole 1116A; 102.14 mbsf. Woody tissue seen in section perpendicular to the stem and preserved as vitrinite. Both the cell walls and the contents have been humified. The cells have probably had additional humic matter added. Reflectances of the cell contents are higher than for the cell walls. Cell walls are dominantly primary cell walls, but local thickening suggests that other tissue may be present. Reflectance contrast between the walls and the contents is strong (reflected light; field width = 0.22 mm; telovitrinite reflectance = 0.40% [cell lumens], 0.18% [walls]). 4. T5855; Hole 1116A; 102.14 mbsf. Both the cell walls and the contents have been humified. The cells have probably had additional humic matter added. Reflectances of the cell contents are higher than for the cell walls. Cell walls include primary cell walls but are sufficiently thick to indicate that some secondary cell wall material must also be present. In the original ICCP terminology, the walls would be termed telinite and the contents collinite. The SAA terminology would place the whole field within the telovitrinite category. Fluorescence of both the cell contents and walls is low (reflected light; field width = 0.22 mm; telovitrinite reflectance = 0.54% [cell lumens], $R = 0.36%$ [cell walls]).



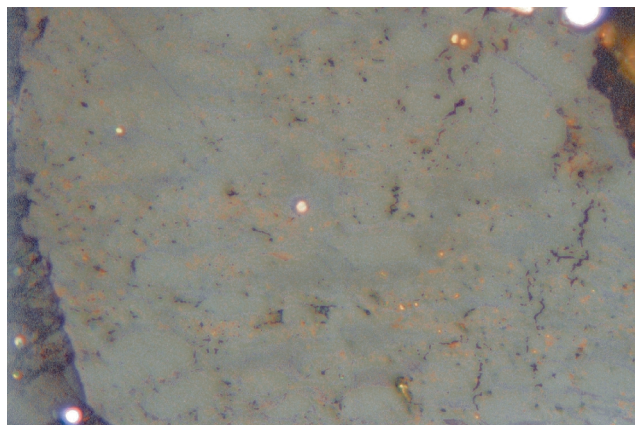
1



2

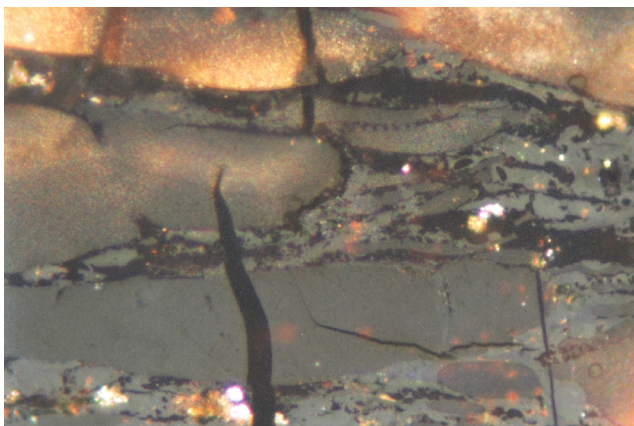


3

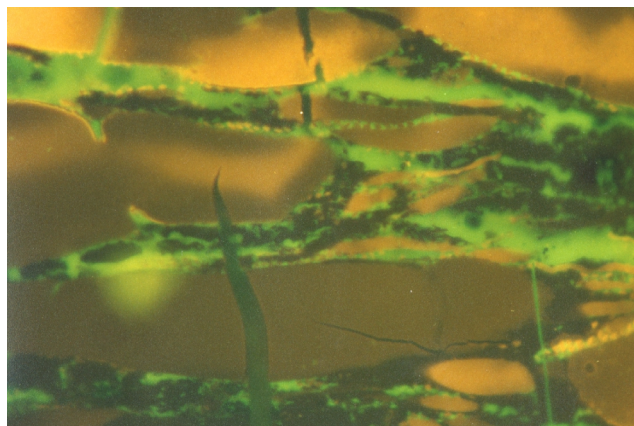


4

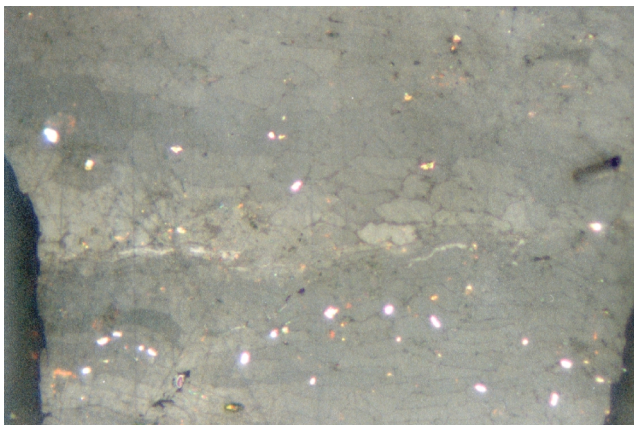
Plate P2. Wood tissues preserved as vitrinite, variable textures, and reflectance. 1. T5848; Hole 1115C; 737.63 mbsf. Woody tissue preserved as vitrinite. Cell lumens are filled with humic material, but the degree of compression is small and some fine structure within the wood is preserved. This sample comes from the deeper part of the sections sampled but is still relatively immature in textural terms. The fractures (black) are the result of desiccation during and after preparation. (reflected light; field width = 0.22 mm; vitrinite reflectance = 0.37%). 2. T5848; Hole 1115C; 737.63 mbsf. Same as figure 1 but in fluorescence mode. Weak fluorescence from the cell contents but stronger fluorescence from some parts of the cell walls, possibly indicating that cellulose or a partial breakdown product of cellulose is still present. Some of the more diffuse brighter patches may represent some show-through from mounting resin below the sample—the vitrinite being relatively translucent (reflected light; field width = 0.22 mm; vitrinite reflectance = 0.37%). 3. T5817; Hole 1109D; 688.21 mbsf. Woody tissue of varying original composition preserved as vitrinite. Cell walls and cell content are both preserved and both show variations in reflectance, but most of the variation is within the cell contents. The variations are present within a single wood fragment and probably relate in large part to wood composition, but these may have been additionally affected by processes active during early diagenesis (reflected light; field width = 0.22 mm; vitrinite reflectance [cell contents] = 0.54%–0.24%). 4. T5817; Hole 1109D; 688.21 mbsf. Woody tissue of varying original composition preserved as vitrinite. Marked variations are present within the telovitrinite, and these are largely due to differences in the original wood composition. Some of the higher reflecting telovitrinite has partial replacement of cell walls by pyrite (reflected light; field width = 0.22 mm; vitrinite reflectance [cell contents] = 0.48% [upper layer] and 0.26% [lower layer]).



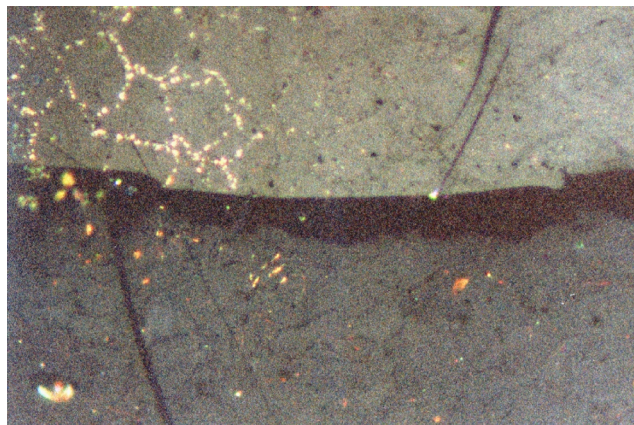
1



2

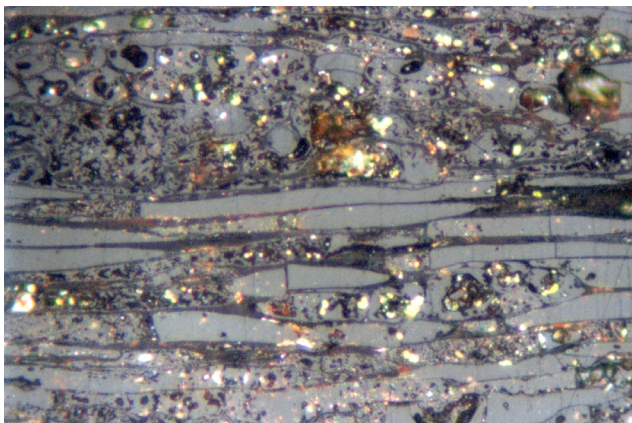


3

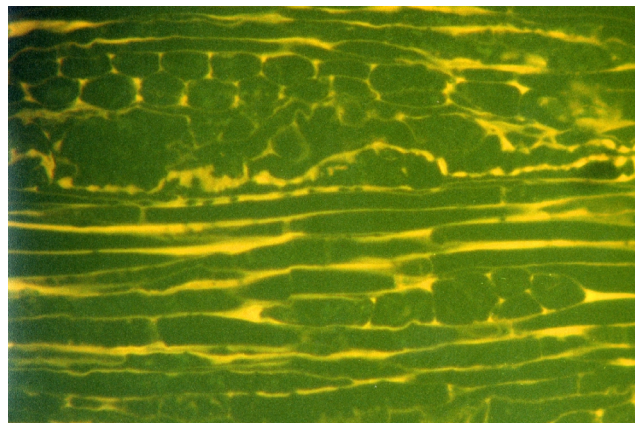


4

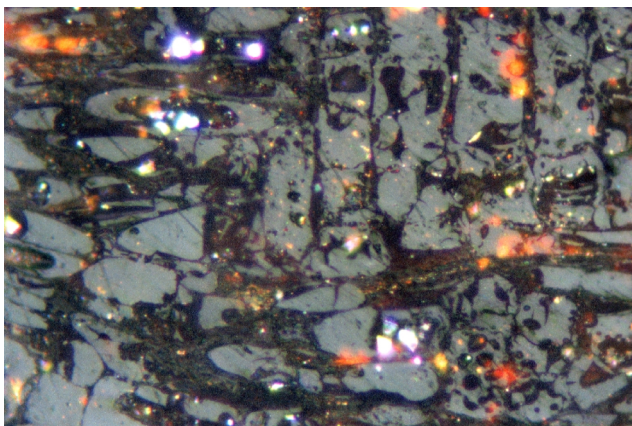
Plate P3. Vitrinite showing fluorescence from cell walls. 1. T5809; Hole 1109D; 387.86 mbsf. Longitudinal section of wood preserved as telovitrinite. The cell lumens are mostly filled with humic material, but the degree of compressions is small and some parts of the lumens are open. Cell walls are much lower in reflectance and are strongly fluorescing. Their reflectances are within the range normally associated with lipinitite, but they do not represent suberinite. Reflectances of the cell walls are lower in the lower part of the field, but the cell contents have relatively consistent reflectances across the various tissue types (reflected light; field width = 0.22 mm; vitrinite reflectance [cell contents] = 0.37%, [cell walls] = 0.12%). 2. T5809; Hole 1109D; 387.86 mbsf. Same as figure 1, but in fluorescence mode. Longitudinal section of wood with the cells outlined by the fluorescence of the cell walls. The structures present are probably xylem, seen in longitudinal section, with some medullary ray tissues in the upper part of the field. Fluorescence of the cell walls is similar to that for suberinite, but the form of the cells shows that this material is not from cork cells and cannot strictly be referred to the maceral suberinite (reflected light; field width = 0.22 mm; vitrinite reflectance [cell contents] = 0.37%, [cell walls] = 0.12%). 3. T5809; Hole 1109D; 387.86 mbsf. Oblique section of wood preserved as telovitrinite. The cell lumens are partially filled with humic material, but open lumens are still present and little compaction has occurred. Cell walls are much lower in reflectance and are most easily seen in fluorescence mode. The vertical cells represent a medullary ray structure (reflected light; field width = 0.22 mm; vitrinite reflectance [cell contents] = 0.34%). 4. T5809; Hole 1109D; 387.86 mbsf. Same as figure 3, but in fluorescence mode. Oblique section of wood preserved as telovitrinite with cell structures outline by fluorescing cell walls. Some structures are probably present within the cell walls, and some fluorescence can be seen from the floors of some cells, with the fluorescence being transmitted through the cell contents (reflected light; field width = 0.22 mm; vitrinite reflectance [cell contents] = 0.34%).



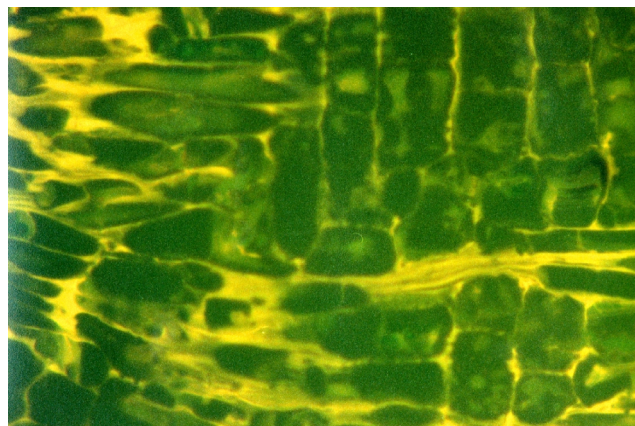
1



2

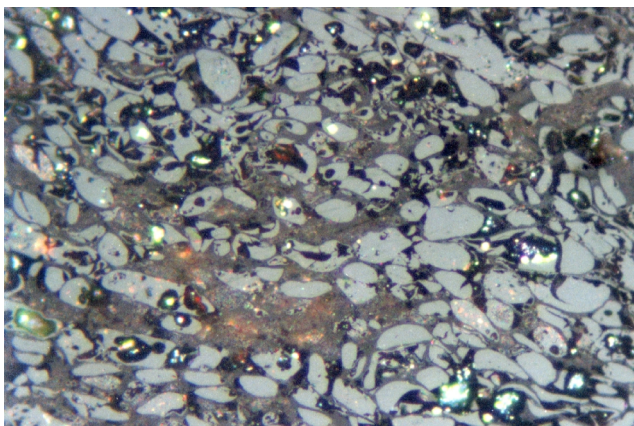


3

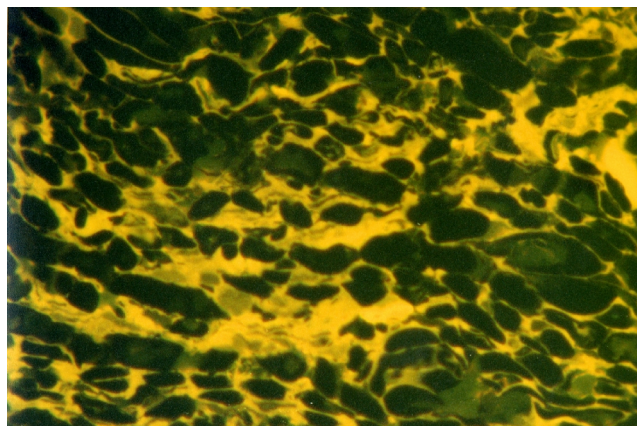


4

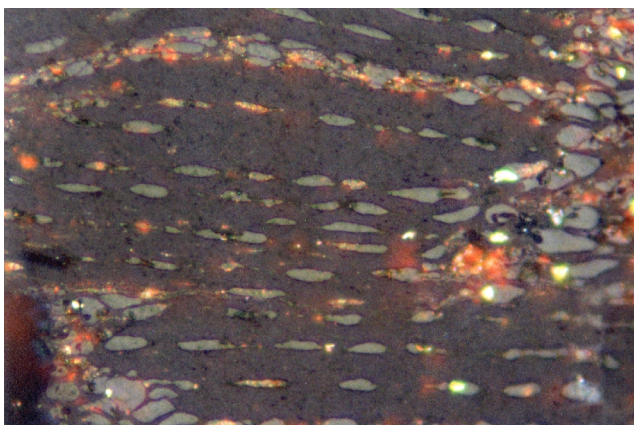
Plate P4. Variable contribution of cell walls to the bulk of vitrinite. 1. T5809; Hole 1109D; 387.86 mbsf. Woody tissue preserved as vitrinite but with the volume of the cell walls close to that of the cell lumens. The corpocollinite within the lumens has a much higher reflectance compared with the cell walls, and its optical properties provide a more reliable measure of coal rank than the optical properties of the cell walls (reflected light; field width = 0.22 mm; vitrinite reflectance [cell contents] = 0.34%). 2. T5809; Hole 1109D; 387.86 mbsf. Same as figure 1, but in fluorescence mode. The cell walls show moderate to strong fluorescence, and moderate positive alteration of the fluorescence was noted on prolonged irradiation. The section is close to being a transverse section of the wood. The larger areas of fluorescence in part indicate sections parallel with a cell wall and in part zones where corpocollinite has not filled the cell lumens (reflected light; field width = 0.22 mm; vitrinite reflectance [cell contents] = 0.34%). 3. T5859; Hole 1118A; 580.69 mbsf. Section of wood where the cell wall material is dominant over the humic corpocollinite cell fillings. In some cases, no cell lumens contain corpocollinite and a much lower reflectance results if all tissues are measured. As far as possible, cell wall materials were excluded from the reflectance data; however, distinction of wall and cell contents is not always as clear as in the fields on this plate (reflected light; field width = 0.22 mm; mean vitrinite reflectance = 0.27%). 4. T5859; Hole 1118A; 580.69 mbsf. Same as figure 3, but in fluorescence mode. Strongly fluorescing cell walls in telovitrinite. The thickness of the cell walls suggests that some secondary cell wall material may be present and that both types of cell wall show similar fluorescence. The color and intensity of the fluorescence is similar to that of suberinite, but the morphology is not that of cork cells (reflected light; field width = 0.22 mm; mean vitrinite reflectance = 0.27%).



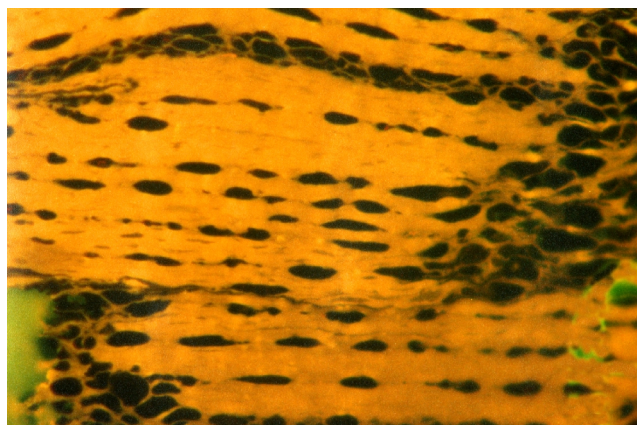
1



2

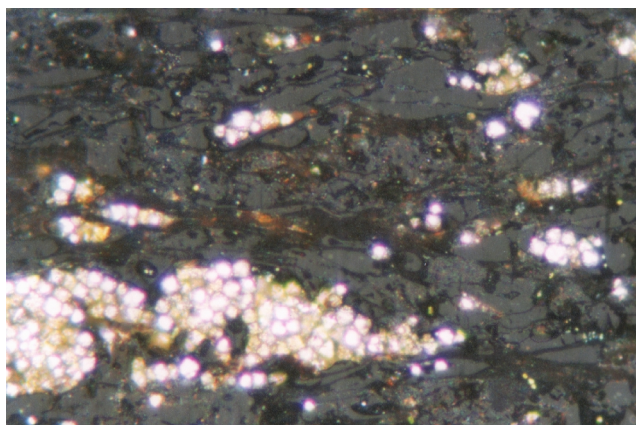


3

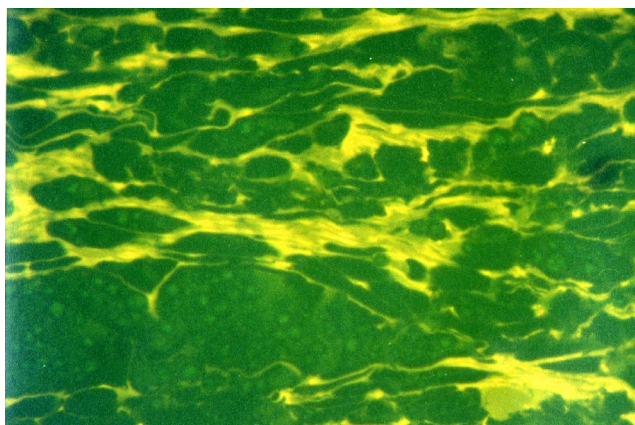


4

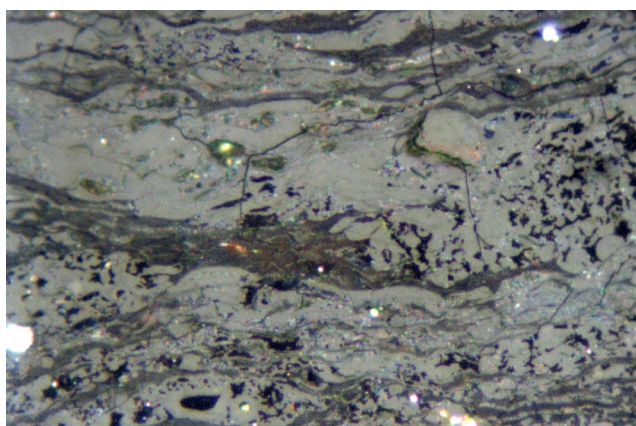
Plate P5. Cell walls transitional to suberinite. 1. T5809; Hole 1109D; 387.86 mbsf. Telovitrinite with fluorescing cell walls and a prominent pyrite lens. Some of the fluorescing tissues are similar to those in Plates P3, p. 24, and P4, p. 25, but some is similar to suberinite (reflected light; field width = 0.22 mm; vitrinite reflectance [cell contents] = 0.31%). 2. T5809; Hole 1109D; 387.86 mbsf. Same as figure 1, but in fluorescence mode. In the upper right of the field the regular stacked structure normally associated with suberinite is present, but in other parts of the field is it lacking, but the cell walls show similar fluorescence properties (reflected light; field width = 0.22 mm; vitrinite reflectance [cell contents] = 0.31%). 3. T5814; Hole 1109D; 551.24 mbsf. Telovitrinite with abundant fluorescing cell walls, some of which are suberinite. The part of the plant that has been preserved is probably part of the periderm, and it appears that multiple periderm layers are present in this wood type. The dark voids are similar in appearance to resinite, but the fluorescence-mode plate shows that resinite is not present and they represent open voids (reflected light; field width = 0.22 mm; mean vitrinite reflectance = 0.39%; suberinite reflectance = 0.18%). 4. T5814; Hole 1109D; 551.24 mbsf. Same as figure 3, but in fluorescence mode. The material most closely referable to suberinite is in the upper right of the field, but this shows weaker fluorescence compared with the cell walls in the center of the field. The structure and fluorescence of some of the layers toward the base of the field are similar to those of cutinite (reflected light; field width = 0.22 mm; vitrinite reflectance = 0.39%, suberinite reflectance = 0.18%).



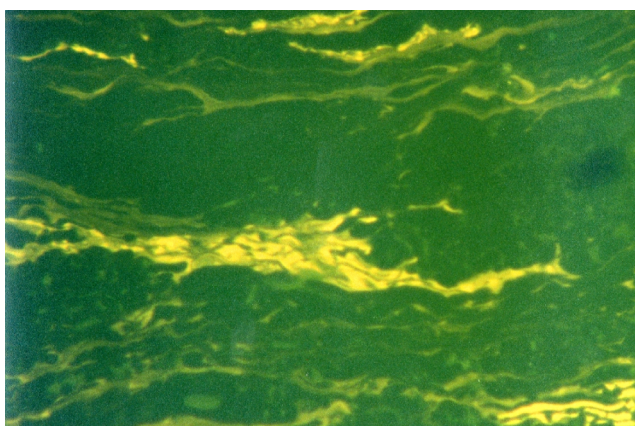
1



2

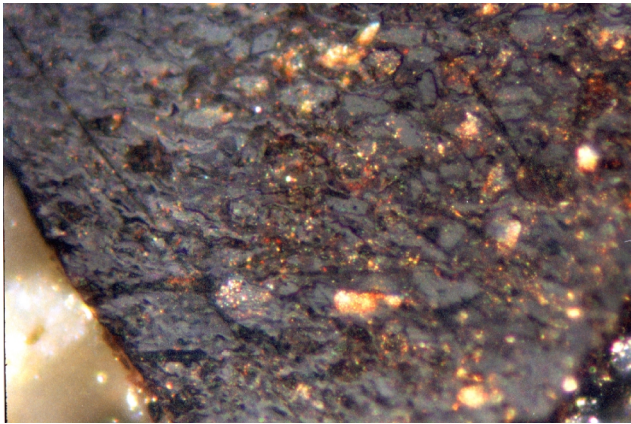


3

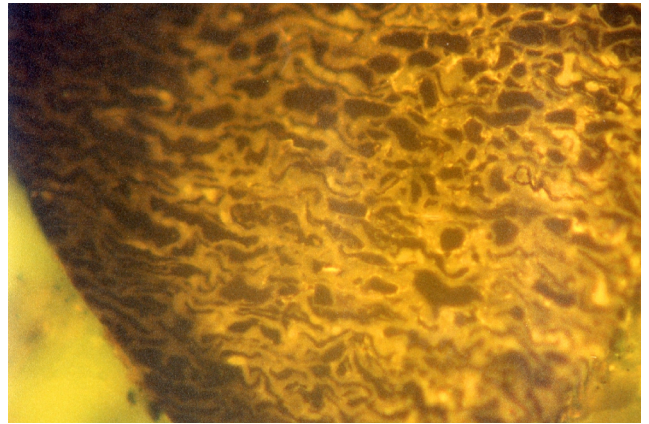


4

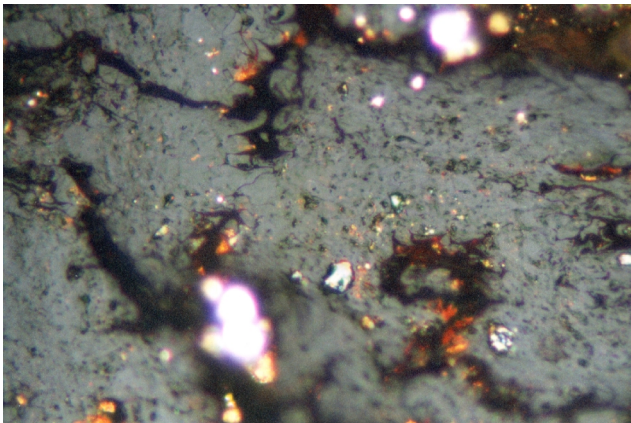
Plate P6. Suberinite and cutinite. 1. T5843; Hole 1115C; 562.86 mbsf. Telovitrinite and suberinite, with the suberinite showing positive alteration on prolonged irradiation with the fluorescence excitation beam. Vitrinite reflectance = 0.32% prior to alteration and 0.26% after 2 hr of irradiation. The left side of the field was not irradiated (reflected light; field width = 0.22 mm; vitrinite reflectance [cell contents] = 0.32%). 2. T5809; Hole 1109D; 387.86 mbsf. Same as figure 1, but in fluorescence mode. Fluorescence from the suberinite is much stronger from the area where alteration has occurred (reflected light; field width = 0.22 mm; vitrinite reflectance [cell contents] = 0.32%). 3. T5822; Hole 1114A; 64.72 mbsf. Telovitrinite with cell structure poorly defined but with cutinite well preserved. The cutinite is difficult to distinguish from desiccation fractures in white light, but is clearly visible in fluorescence mode (reflected light; field width = 0.22 mm; mean vitrinite reflectance = 0.33%). 4. T5822; Hole 1114A; 64.72 mbsf. Same as figure 3, but in fluorescence mode. Cutinite probably seen is section oblique to the surface of the wood. The section angle has emphasized small reentrants within the outer layers. Fluorescence of the cutinite is strong, and the form indicates that it is associated with wood rather than leaf tissues (reflected light; field width = 0.22 mm; mean vitrinite reflectance = 0.33%).



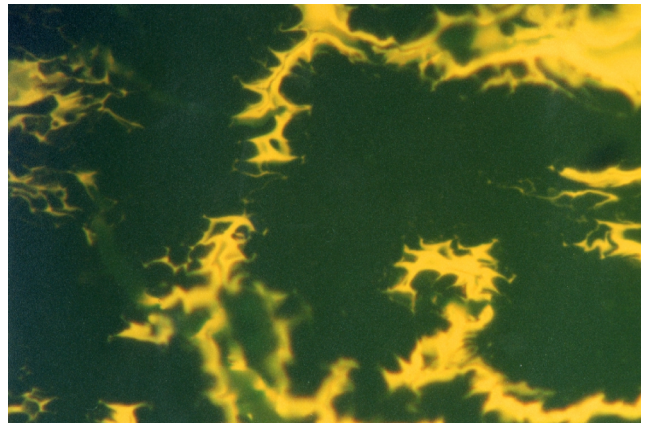
1



2

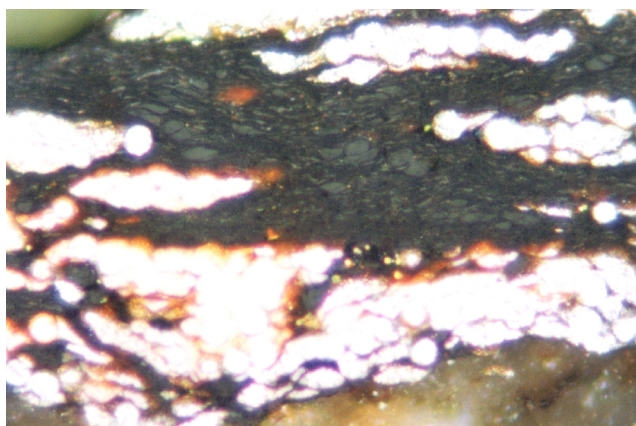


3

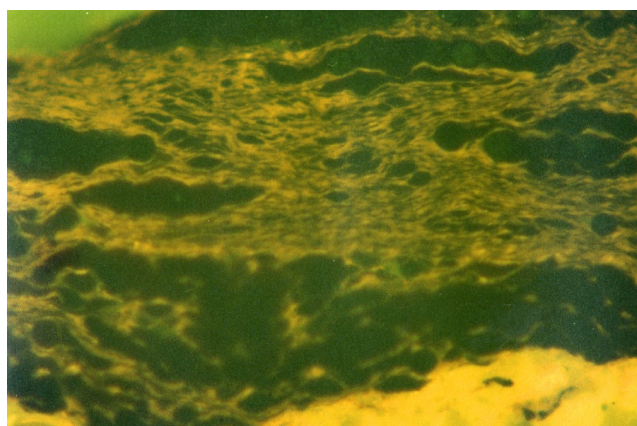


4

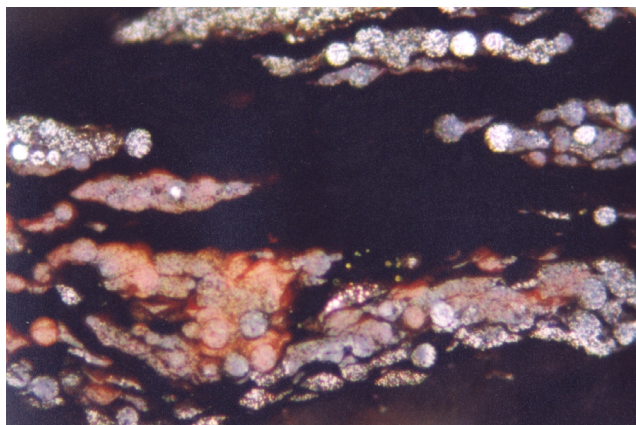
Plate P7. Vitrinite, pyrite, and oil inclusions. 1. T5863; Hole 1118A; 744.27 mbsf. Telovitrinite with fluorescing cell walls and abundant layers of pyrite. This plate has been exposed to illustrate the vitrinite and figure 3 to show the pyrite (reflected light; field width = 0.22 mm; mean vitrinite reflectance = 0.36%). 2. T5863; Hole 1118A; 744.27 mbsf. Telovitrinite with fluorescing cell walls and abundant layers of pyrite. The pyrite appears dark in fluorescence mode, and the small fluorescing areas within the pyrite lenses may represent remnant plant structures that have been largely replaced by pyrite (reflected light; field width = 0.22 mm; mean vitrinite reflectance = 0.36%). 3. T5863; Hole 1118A; 744.27 mbsf. Telovitrinite with fluorescing cell walls and abundant layers of pyrite. This plate has been exposed to illustrate the pyrite. The brighter areas are unaltered pyrite, but most of the original framboidal pyrite has been altered to iron oxides. It is thought that this alteration has occurred during drying of the sample and indicates that the pyrite is highly reactive (reflected light; field width = 0.22 mm; mean vitrinite reflectance = 0.36%). 4. T5842; Hole 1115C; 514.72 mbsf. Oil drops within siltstone. These oil drops are relatively rare in the sample suite. Some occurrences are probably contaminants, but these appear to be indigenous to the sample. Light paraffinic oils have this appearance in fluorescence mode (reflected light; field width = 0.22 mm; mean vitrinite reflectance = 0.29%).



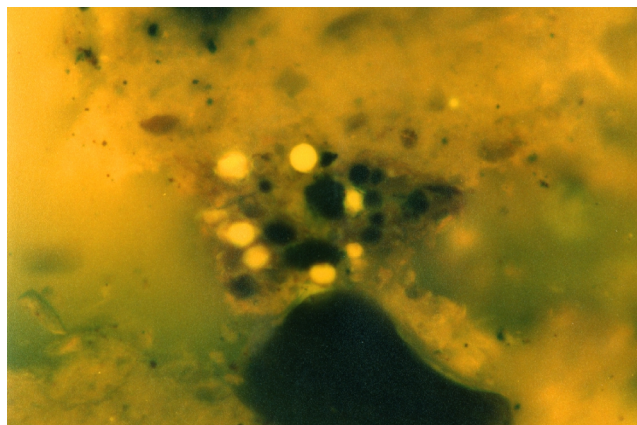
1



2

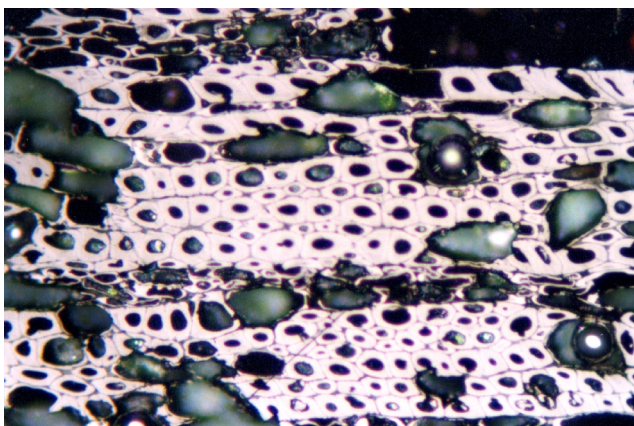


3

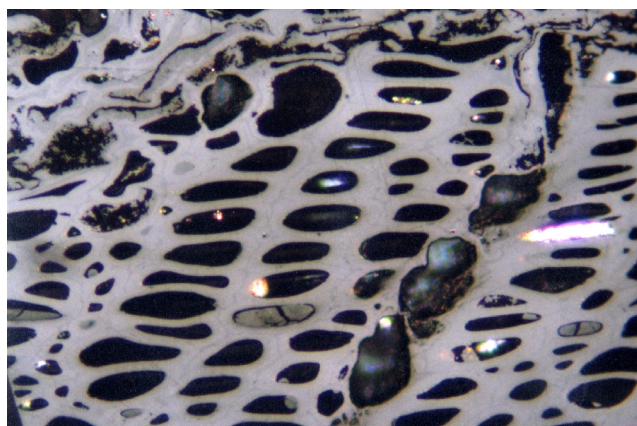


4

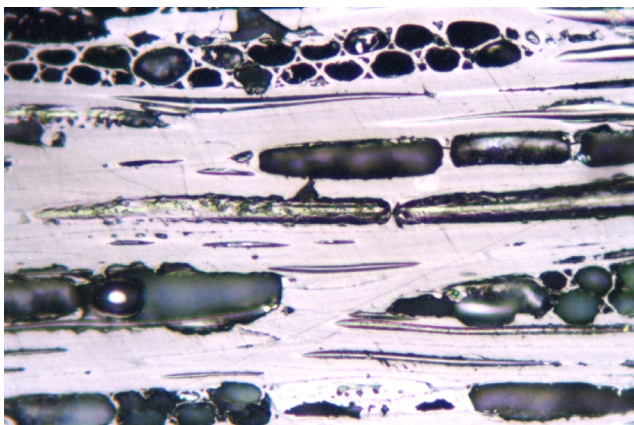
Plate P8. Pyrofusinite and pyrite replacement of woods. 1. T5829; Hole 1115A; 272.84 mbsf. Fusinite formed by charring of woody tissues. Fusinite is generally absent from the sample suite but is dominant in two samples. In these samples, probable air-fall tuff fragments are present, but such tuff fragments are present in many samples lacking fusinite. Reflectance of secondary cell walls = 3.46%. Primary cell walls have a much lower reflectance but are too thin to measure accurately (reflected light; field width = 0.22 mm; mean vitrinite reflectance = 0.22% and 0.25% in adjacent samples). 2. T5859; Hole 1118C; 725.88 mbsf. Material close to the fusinite to semifusinite boundary but formed by the charring of woody tissues. Some commercially available artificial chars show reflectance down to 0.7%. Reflectance of secondary cell walls = 1.10%. As for figure 1, the primary cell walls have a lower reflectance than the secondary walls (reflected light; field width = 0.22 mm; mean vitrinite reflectance = 0.33% and 0.28% in adjacent samples). 3. T5829; Hole 1115A; 272.84 mbsf. Fusinite formed by charring of woody tissues, in this case xylem tissues, seen in longitudinal section. Cell wall structures are preserved, and some probable pit structures, probably scalariform pitting, are seen in some of the cell lumens. Reflectance of secondary cell walls = 3.96%. Primary cell walls seem to be similar to the secondary cell walls in terms of reflectances in this field (reflected light; field width = 0.22 mm; mean vitrinite reflectance = 0.22% and 0.25% in adjacent samples). 4. T5840; Hole 1115C; 489.50 mbsf. Pyrite petrification of wood tissue. The darker areas are cell walls preserved as vitrinite. The tissue is xylem seen in longitudinal section, and the vertical structures are medullary rays (reflected light; field width = 0.22 mm; mean vitrinite reflectance = 0.29%).



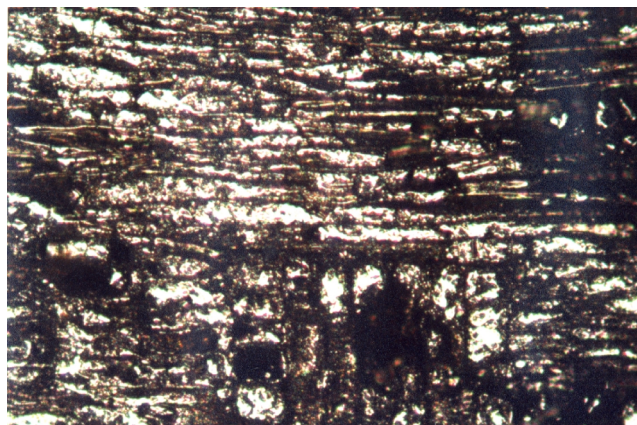
1



2

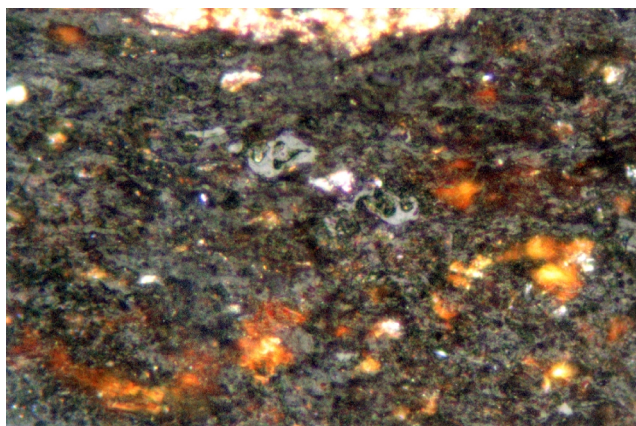


3

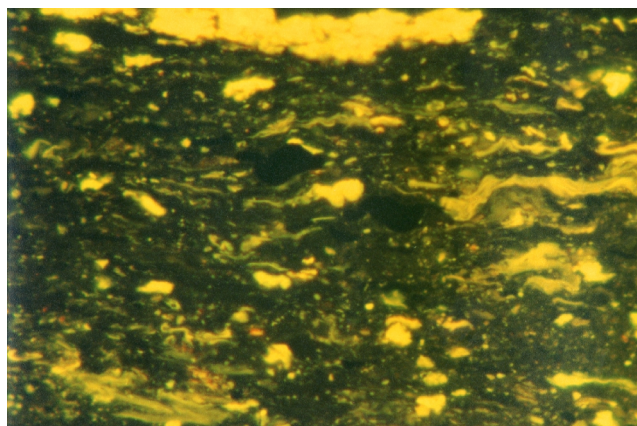


4

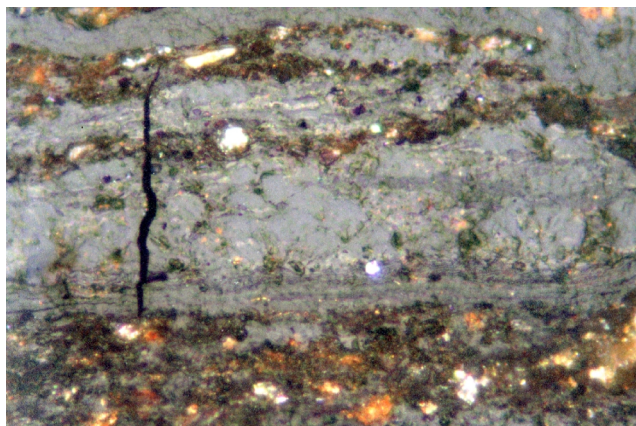
Plate P9. Coal and shaly coal. 1. T5818; Hole 1109D; 969.89 mbsf. Shaly coal. Possible in situ roots are present in some horizons, but in Hole 1109D some of the deeper samples represent hypautochthonous peats. It is possible that these samples represent intraclasts, but an indigenous origin is more probable. This field shows a shaly coal with detrovitrinite, resinite, sporinite, and liptodetrinite. Liptinite-rich horizons such as this are typical of peat swamps but not of fringing marine settings in the Tertiary (reflected light; field width = 0.22 mm; detrovitrinite reflection = 0.30%). 2. T5818; Hole 1109D; 969.89 mbsf. Same as figure 1, but in fluorescence mode. Shaly coal with detrovitrinite, resinite, sporinite, and liptodetrinite (reflected light; field width = 0.22 mm; detrovitrinite reflection = 0.30%). 3. T5818; Hole 1109D; 969.89 mbsf. Coal with telovitrinite, detrovitrinite, resinite, sporinite, and liptodetrinite. The telovitrinite contains some weakly fluorescing tissues that probably represent periderm, and the telovitrinite may be derived from root tissues. The textures and maceral composition are not those typical of mangrove/Nypa swamps, and it is more likely that this peat was formed in an inland setting (reflected light; field width = 0.22 mm; telovitrinite reflection = 0.30%). 4. T5818; Hole 1109D; 969.89 mbsf. Same as figure 3, but in fluorescence mode. The telovitrinite shows weak fluorescence from some layers, and the resinite, sporinite, and liptodetrinite all show intense yellow fluorescence. The weakly fluorescing tissues may represent suberin-like layers or could have affinities to cutinite (reflected light; field width = 0.22 mm; telovitrinite reflection = 0.30%).



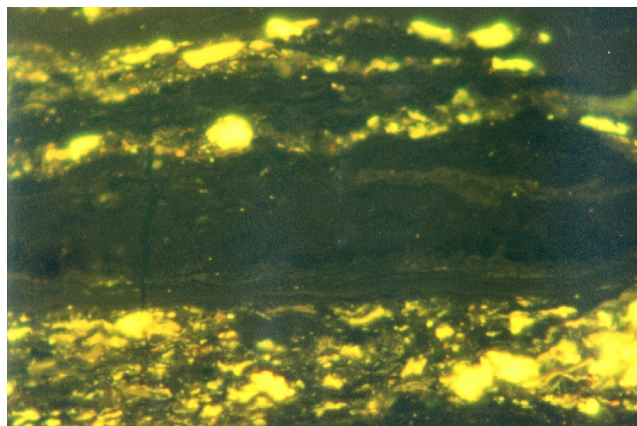
1



2

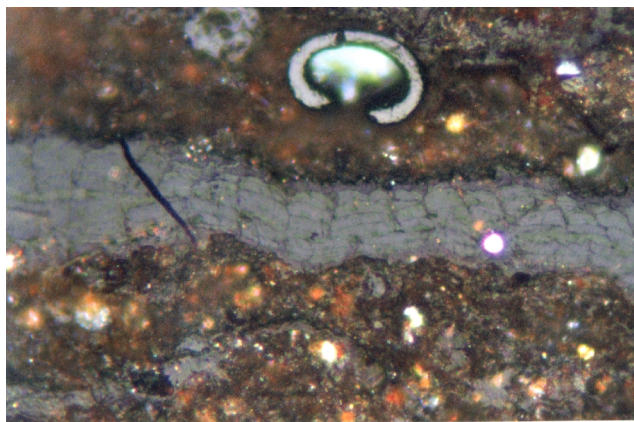


3

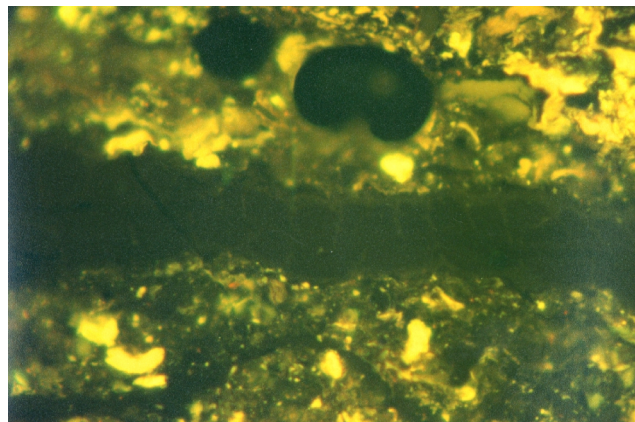


4

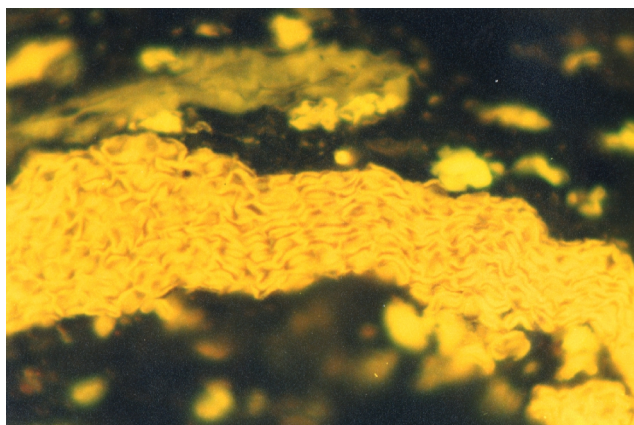
Plate P10. Coal and shaly coal–cork cells and suberinite. 1. T5818; Hole 1109D; 969.89 mbsf. Shaly coal with a prominent layer of telovitrinite showing cork cell structures. The horseshoe-shaped white entity is a broken fungal teleutospore. Small amounts of pyrite suggest some marine influence, but this could be postdepositional. Smaller amounts of degraded telovitrinite and detrovitrinite are present, and abundant liptinite is seen in the fluorescence-mode plate (reflected light; field width = 0.22 mm; telovitrinite reflectance = 0.28%, teleutospore reflectance = 0.46%). 2. T5818; Hole 1109D; 969.89 mbsf. Same as figure 1, but in fluorescence mode. The outlines of the cell structures within the telovitrinite are weakly shown by fluorescence from the primary cell walls. Note that fluorescence from these cork cell tissues is less intense than that from normal woody tissues in many of the earlier plates. Abundant liptinite is present within the clay-rich layers and has affinities to resinite and suberinite (reflected light; field width = 0.22 mm; telovitrinite reflectance = 0.28%; teleutospore reflectance = 0.46%). 3. T5818; Hole 1109D; 969.89 mbsf. Strongly fluorescing layer that appears to represent suberinite, although in general appearance it is similar to a sporangium. Polishing hardness is relatively high (reflected light; field width = 0.22 mm; mean vitrinite reflectance = 0.28% for sample). 4. T5818; Hole 1109D; 969.89 mbsf. Strongly fluorescing suberinite seen in section approximately parallel with the surface of the wood. The typical oblong shape of cork cell is seen, and a compound cell wall structure can be resolved. This consists of a weakly fluorescing middle lamella flanked by more strongly fluorescing secondary cell walls. The secondary cell walls are thicker but are thin compared with the secondary cell walls of some cell types; see, for example, Plate P8, p. 29 (reflected light; field width = 0.22 mm; mean vitrinite reflectance = 0.28% for sample).



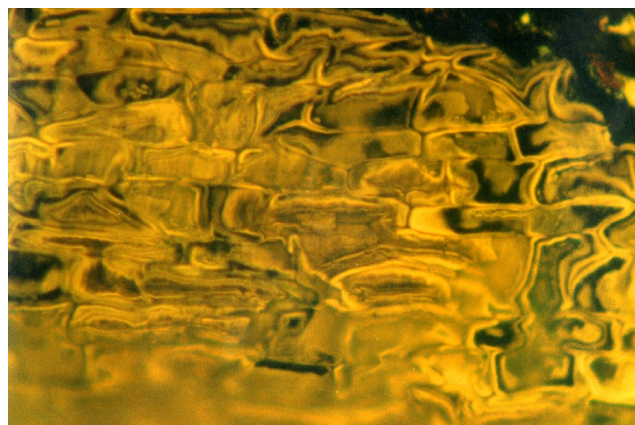
1



2

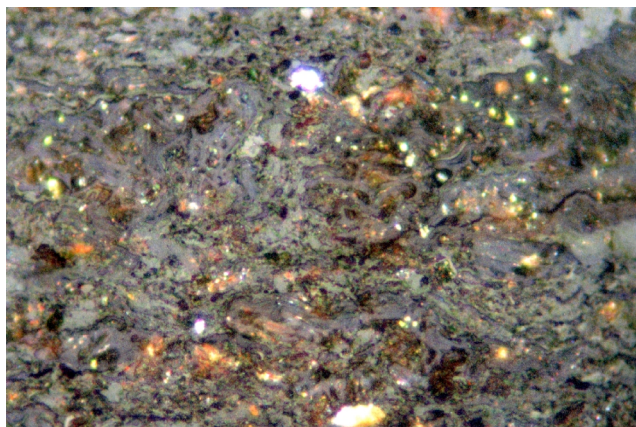


3

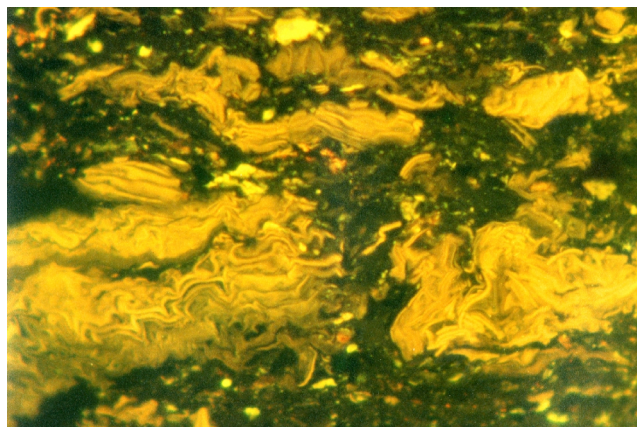


4

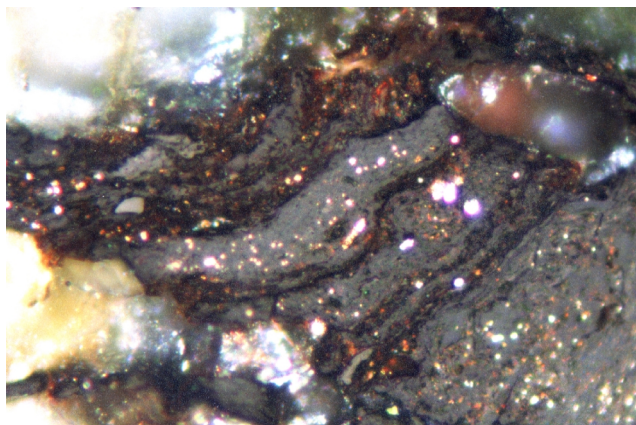
Plate P11. Coal and coal intraclasts. 1. T5818; Hole 1109D; 969.89 mbsf. Coal with major vitrinite that appears to represent structured telovitrinite, but is seen from figure 2 to represent numerous broken fragments of bark tissues mixed with degraded wood. Small pyrite framboids indicate some marine influence (reflected light; field width = 0.22 mm; vitrinite reflectance = 0.30%). 2. T5818; Hole 1109D; 969.89 mbsf. Same as figure 1, but in fluorescence mode. Strongly fluorescing suberinite seen in various section ranging from parallel with the surface of the wood to longitudinal section and in cross section. Small amounts of resinite are present in the groundmass together with liptodetrinite (reflected light; field width = 0.22 mm; vitrinite reflectance = 0.30%). 3. T5856; Hole 1116A; 110.93 mbsf. Peat intraclast with thin telovitrinite layers and resinite. The bedding within the sediment is horizontal. Abundant pyrite is present. The pyrite deposition could have occurred during the reworking and deposition within a probable marine setting (reflected light; field width = 0.22 mm; telovitrinite reflectance = 0.42%). 4. T5856; Hole 1116A; 110.93 mbsf. Same as figure 3, but in fluorescence mode. Peat intraclast with the intraclast bedding outlined by the laminae rich in resinite. Smaller amounts of resinite are dispersed within the matrix of the siltstone (reflected light; field width = 0.22 mm; telovitrinite reflectance = 0.42%).



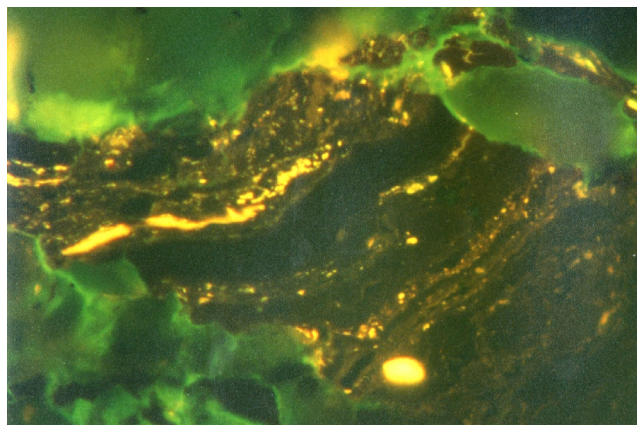
1



2

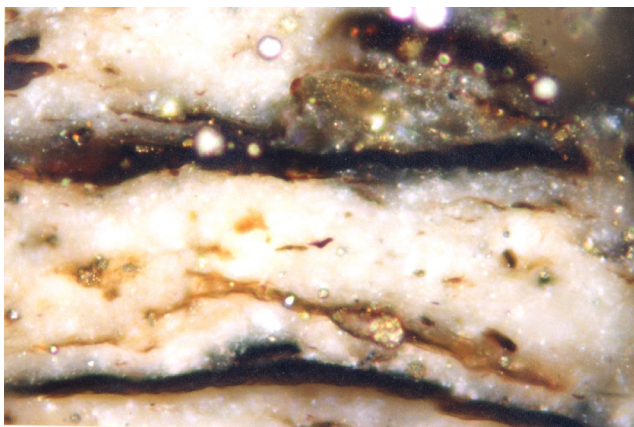


3

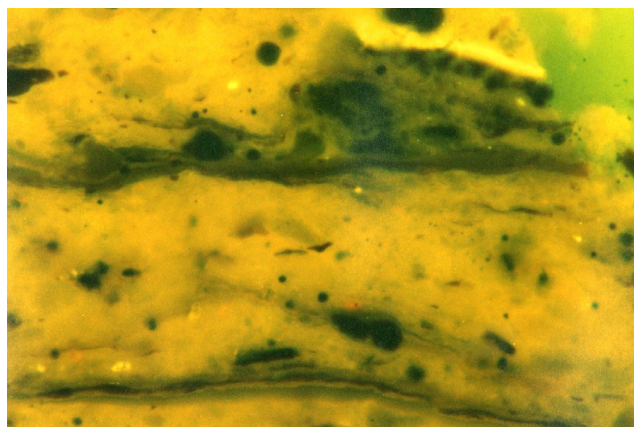


4

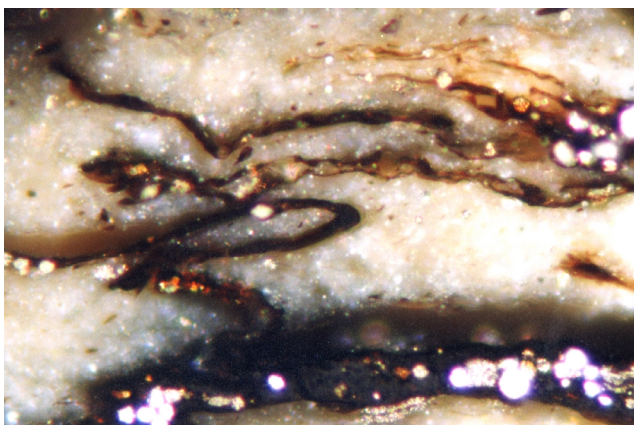
Plate P12. Dispersed organic matter. 1. T5842; Hole 1115C; 514.24 mbsf. Claystone with abundant plant fragments (DOM). In this field most appear to have affinities with liptinite but a few show strong fluorescence (reflected light; field width = 0.22 mm; vitrinite reflectance = 0.30%). 2. T5842; Hole 1115C; 514.24 mbsf. Same as figure 1, but in fluorescence mode. Claystone with abundant plant fragments (DOM). In fluorescence mode the DOM can be seen to be cutinite, but fluorescence ranges from very weak (two longer occurrences) to moderate, short fragments (upper right) (reflected light; field width = 0.22 mm; vitrinite reflectance = 0.30%). 3. T5842; Hole 1115C; 514.24 mbsf. Claystone with abundant DOM. The lower lens is vitrinite, probably telovitrinite, but the upper fragments are mainly of cutinite. These have a very low reflectance and are partially translucent. The organic matter is associated with pyrite (reflected light; field width = 0.22 mm; vitrinite reflectance = 0.30%). 4. T5856; Hole 1116A; 110.93 mbsf. Same as figure 3, but in fluorescence mode. Some structures within the vitrinite may show weak fluorescence, but the cutinite either shows very weak fluorescence or none. It is possible that the small amount of light from the cutinite represents show-through from underlying mineral fluorescence, but the morphology of the phytoclasts is clearly that of cutinite (reflected light; field width = 0.22 mm; telovitrinite reflectance = 0.42%).



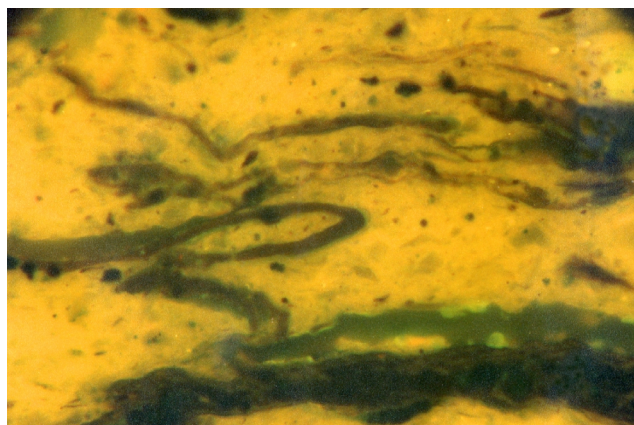
1



2

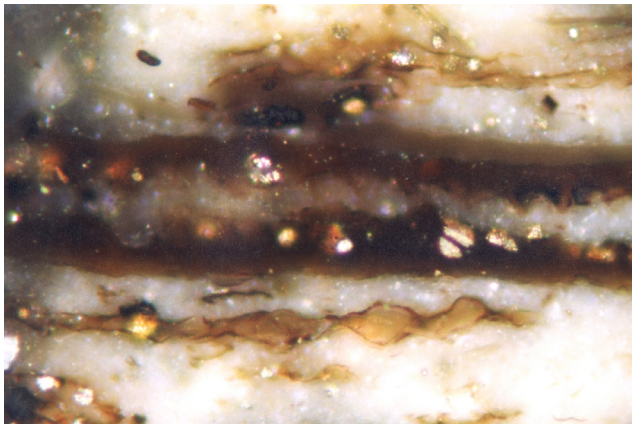


3

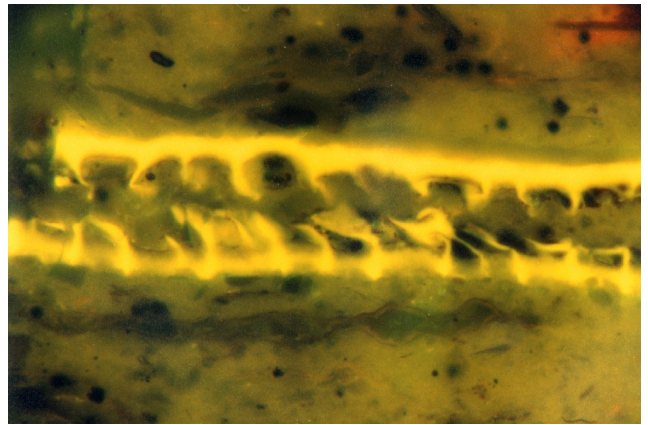


4

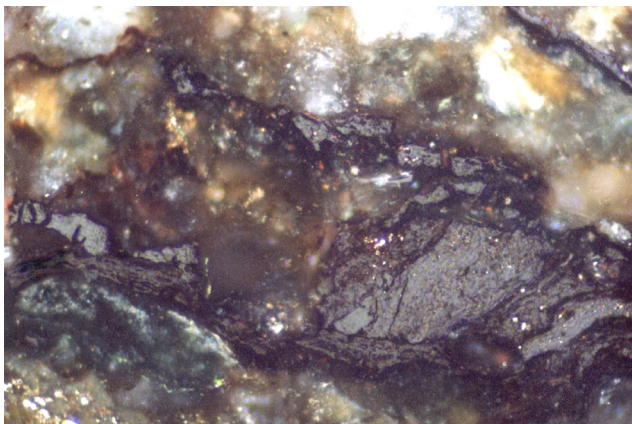
Plate P13. Dispersed organic matter. 1. T5842; Hole 1115C; 514.24 mbsf. Leaf preserved in claystone. The leaf no longer contains the tissues within the cuticle (mesophyll tissue). However, these must have been there at the time of deposition, otherwise the two cuticle surfaces would have tended to be torn apart. Subsequent diagenesis has apparently removed these tissues. The amber-colored wisps are probably also derived from leaf tissue (reflected light; field width = 0.22 mm; mean vitrinite reflectance = 0.29%). 2. T5842; Hole 1115C; 514.24 mbsf. Same as figure 1, but in fluorescence mode. The smooth surfaces of the cutinite represent the outer leaf surfaces, and the inner saw-toothed appearance is typical of leaf cuticles. The projection bounds the palisade cells. Commonly, palisade cells are preserved as vitrinite, and their absence in this occurrence suggests strong biochemical decay has occurred, leaving the relatively refractory cuticle intact (reflected light; field width = 0.22 mm; mean vitrinite reflectance = 0.29%). 3. T5856; Hole 1116A; 110.93 mbsf. DOM comprising telovitrinite that appears to represent in situ root tissue. Elongate structures such as these do not normally remain intact during transport. Therefore, an in situ origin is likely (reflected light; field width = 0.56 mm; mean vitrinite reflectance = 0.34%). 4. T5856; Hole 1116A; 110.93 mbsf. Elongate and anastomosing occurrences of telovitrinite that appear to represent in situ root tissue. Elongate structures such as these do not normally remain intact during transport. Therefore, an in situ origin is likely. Pyritization of the vitrinite has occurred (reflected light; field width = 0.56 mm; mean vitrinite reflectance = 0.34%).



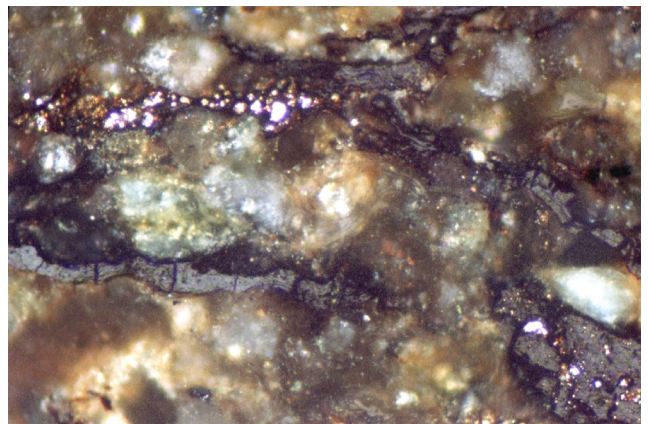
1



2

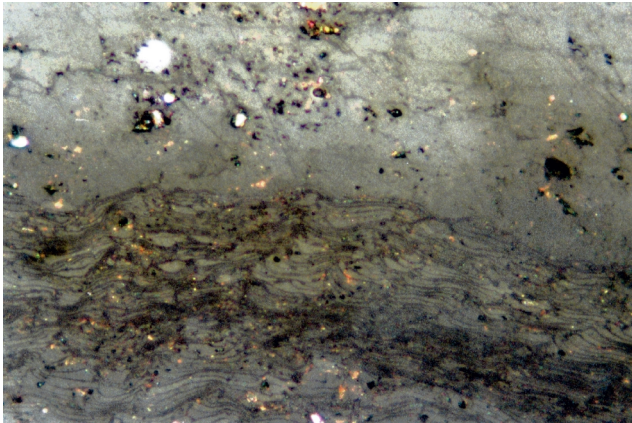


3

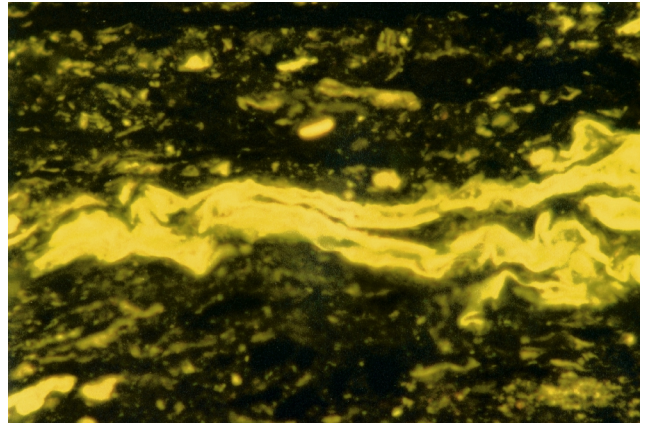


4

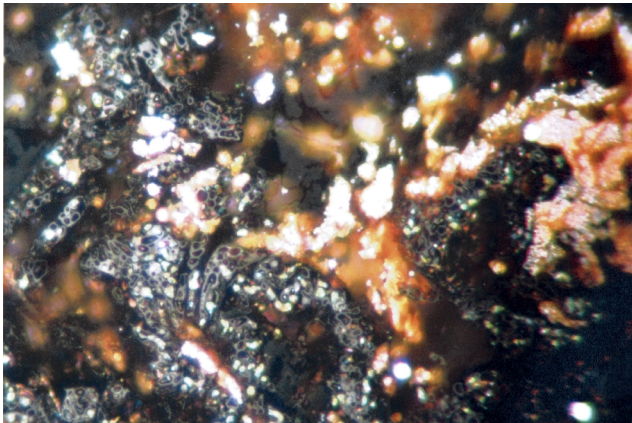
Plate P14. Suberinite, fungal tissues. 1. T5819; Hole 1116D; 703.23 mbsf. Fungal resting spore (sclerotium). Occurrences of sclerotia and teleutospores are highly characteristic of Tertiary and Holocene coals and, to a lesser extent, organic-rich sediments. Although similar fungi were present at earlier times, these highly chitinized bodies were not preserved (reflected light; field width = 0.22 mm; mean vitrinite reflectance = 0.39%; sclerotinite reflectance = 1.20%). 2. T5828; Hole 1115D; 241.48 mbsf. Telovitrinite (dark gray) with abundant pale gray fungal hyphae invading the tissues. Fungal attack is common, but the hyphae do not always show optical contrast as strong as in this field (reflected light; field width = 0.22 mm; mean telovitrinite reflectance = 0.15%; fungal tissue reflectance = 0.66%). 3. T5818; Hole 1109D; 696.89 mbsf. Prominent layer of strongly fluorescing suberinite is shaly coal. The dark layers and lenses are vitrinite, and abundant resinite and liptodetrinite are also present (reflected light; field width = 0.22 mm; mean vitrinite reflectance = 0.28%). 4. T5817; Hole 1109D; 688.21 mbsf. Wood tissue showing the outer layers with suberinite present in the upper part of the field and gelified tissue in the lower part of the field (reflected light; field width = 0.22 mm; mean vitrinite reflectance = 0.40%).



1



2



3



4